J Solid State Electrochem (2002) 6: 145–164
DOI 10.1007/s100080100219

REVIEW

Patrik Schmuki

# From Bacon to barriers: a review on the passivity of metals and alloys

Received: 13 November 2000 / Accepted: 23 March 2001 / Published online: 13 June 2001


**Abstract** Passivity of metals and alloys is a phenomenon of utmost technical importance as it prevents many construction materials from rapid deterioration. For the majority of metals, passivity is based on the spontaneous formation of a thin oxide layer (the passive film), in a specific environment. This film can slow corrosion (dissolution) reactions by many orders of magnitude. The present review tries to give an overview of several important aspects and factors that influence film formation, stability and breakdown. Emphasis is on chemical stability and its connection to thermodynamic, kinetic and electronic aspects of the metal/oxide/environment system. Although some metals (e.g. Fe) and alloys (e.g. Fe/Cr) are treated with greater depth, the focal point is the description of general mechanistic approaches – for specific systems the reader is referred to secondary literature.

**Keywords** Passivity · Passive film · Film growth · Corrosion · Pitting

## Introduction

Over the centuries many philosophers have spent considerable thought on the decay and "gnawing away" of matter and the prevention of this seemingly natural process. A key figure in this respect was Francis Bacon (1561–1626), one of the philosophers of the "New Science" and opponent of Aristotle. Whereas Aristotle considered rust to be simply a normal part of earthly decay – all things on earth are slated to pass away – in opposition to the perfection of the heavens, Bacon discussed rust under the more general topic of "The History of Dense and the Rare", the latter being the study of the rather general property of dilation or rarefaction [1, 2]. In this context, Bacon tells us that just as frogs swell when they are angry, so too, "In all decay and putrefaction the native spirits of the body begin to swell; and when they hasten to come forth, they loosen and alter the framework of the body. In like manner rust is formed on metals, glass and the like, from a dilation of the native spirit, which swells, and presses on the grosser parts, driving and propelling them before it that it may get out." In other words, the cause of rust is internal; what we see on the surface is the expression of a process that begins much deeper. Moreover, the difference between organic and inorganic processes is, in this case, negligible.

Fortunately, we know meanwhile that although "Things must go" there are mechanisms that slow down this process dramatically. In the case of metal corrosion such an effect, the phenomenon of passivity, was discovered in the eighteenth century in iron dissolution experiments by Lomonossow [3], Wenzel [4], and Keir [5] and was named "passivity" in 1836 by Schönbein [6]. It described the experimental finding that a thermodynamically expected metal dissolution reaction under certain conditions is kinetically hindered by orders of magnitude. As in many other instances of scientific innovation, technical understanding – the know-how – preceded scientific understanding – the know-why – of the phenomenon. In the case of passivity, for example, it was already known by 1911 that alloying chromium to iron leads to a radically improved corrosion resistance of the alloy [7]. This was immediately applied in the manufacturing of cutlery; however, it took another 50 years for researchers to understand that passivity is based on the spontaneous formation of a highly protective oxide film, the passive film, on the metal surface, as it reacts with the environment. These films, which in many cases are no thicker than only a few nanometers, act as a reactivity barrier between the metal surface and the aggressive environment.

It has been established that the quality of the film in terms of the ion- and electron-transport properties, or

P. Schmuki
University of Erlangen-Nuremberg,
Department of Materials Science, LKO,
Martensstrasse 7, 91058 Erlangen, Germany
E-mail: schmuki@ww.uni-erlangen.de

in terms of its structure and chemistry, determines the dissolution rate of passive metals in a specific environment. This is, of course, of enormous technological significance, since the dissolution rate often determines the lifetime of structural materials. In industrialized countries, the cost of corrosion is estimated to be about 3.5% of the gross national product. Areas such as construction materials, electronics, and transportation are affected and thus any measure that enhances the passive state may also have a considerable economic impact.

Since the discovery of passivity, the nature of the passive film and the factors influencing its properties and behavior have been discussed in a large number of articles (for fundamentals of corrosion and passivity see Ref. [8]). Interest in the phenomenon is further reflected in the continuous series of "Passivity" meetings [9, 10, 11, 12, 13, 14, 15, 16], numerous Passivity symposia of the Electrochemical Society and the International Society of Electrochemistry, etc.

Not only the passivation of metals but also the passivation of semiconductors (particularly on Si, GaAs, InP) is a subject of intense investigation. Often, the goal is not the suppression of corrosion but either the formation of a dielectric layer that can be exploited for devices (metal/insulator/semiconductor structures) or to minimize interface states (dangling bonds) on the semiconductor surface [17, 18] and thus to improve the performance of a microelectronic device. Thin oxide films are also of great significance in batteries, electrocatalysis or for surface patterning. This review, however, will focus on the passivity of metals and its role in corrosion protection, first addressing some general fundamentals, and then giving a brief overview of specific examples of technically important materials.

## Fundamentals of passivity

### Passive film formation

For a metal exposed to a solution or air, thermodynamic stability is generally only provided for noble metals as their oxidation potential is more anodic than the reduction potential of species commonly occurring in the surrounding phase. For nonnoble metals the situation is reversed; the difference in red/ox potentials of the two phases in contact leads to a driving force for metal oxidation. The environmental conditions then can either favor dissolution (solvation) of the oxidized metal cation (active corrosion) according to Eq. (1) or the formation of a second phase film – usually an insoluble 3D surface oxide film (passivation) – according to Eq. (2):

$$M \underset{H_2O}{\overset{-e}{\leftrightarrow}} M(OH) \underset{H_2O}{\overset{-e}{\leftrightarrow}} MOH^{+} \underset{H_2O}{\leftrightarrow} M(H_2O)_6^{2+}(\text{active dissolution}) - e \updownarrow H_2O \quad (1)$$

$$(OH)_2 \leftrightarrow MO \quad (\text{passivation}) \quad (2)$$

In this sense, active dissolution and passivation are competing reactions.

Since passivation reactions involve electrochemical steps, it is often convenient to study active/passive transitions by electrochemical methods such as potentiodynamic polarization curves (Fig. 1). In terms of an electrochemical treatment, passivation of a surface represents a significant deviation from ideal electrode behavior. Passivation is manifested in a polarization curve (Fig. 1, solid line) by a dramatic decrease in current at a particular onset potential (the passivation potential, $U_p$). The corrosion reaction rate, i.e., the anodic current density is lowered by several orders of magnitude. A measure for the "easiness" of passivation, frequently used in the literature, is the critical current density ($i_{cr}$), i.e., the maximum current density reached in the active/passive transition.

Generally, the reaction scheme for passivation can be divided into active range, transition range, prepassive range, and passive layer formation [19, 21]. In the transition and prepassive range the metal becomes increasingly covered by $M(OH)_x$ adsorbates. These adsorbates increasingly block the active dissolution (apparent in polarization curves as a deviation from the active dissolution behavior). The passivation potential is reached when the surface is completely covered with adsorbates and deprotonization leads to the formation of a primary passivating film that mainly consists of $MO_x$ (the valency of the metal cations depends on the metal and the passivation conditions).

Passivation of many metals and alloys typically takes place through the formation of such oxide films, whose composition and thickness vary with potential, time, temperature, and environmental composition. An

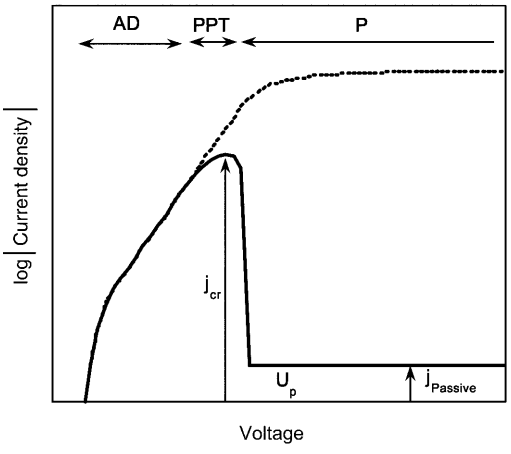


**Fig. 1** The *solid line* shows a typical anodic polarization curve for a metal electrode exhibiting passivation at a distinct anodic potential, $U_p$. The different regions correspond to active dissolution (*AD*), the prepassive and transition range (*PPT*), and stable passivation (*P*). The current flow in the passive range ($i_{Passive}$) is a measure for the protectiveness or the quality of the oxide film. For comparison, the *dashed line* represents the polarization behavior of a nonpassive metal showing AD over the entire anodic potential range. At high potentials, where the current becomes independent of the potential, dissolution of the metal occurs through a salt layer

extensive analysis of the active/passive transition of the iron group metals can be found in Ref. [22].

*Thermodynamics*

The value and existence of a passivation potential is based on the thermodynamics of oxide formation. The results of calculations for the thermodynamic stability of different species considered in electrochemical reactions are frequently represented as pH–potential diagrams (so-called Pourbaix diagrams [23]). The Pourbaix diagram for iron in an aqueous environment is shown in Fig. 2. The diagram gives regions of existence, i.e., for a particular combination of pH and red/ox potential it can be predicted whether it is thermodynamically favorable for, example, iron to be inert (stable) (region A), to actively dissolve (region B), or to form an oxide layer (region C). Accordingly, passivation potentials and conditions for oxide formation can be predicted. A polarization curve as in Fig. 1 can be perceived as reflecting a cross section through the Pourbaix diagram at a fixed pH. For example, at pH 7 one crosses, moving from cathodic to anodic potentials, first the active metal dissolution line (I), then the passivation line (II) at $U_p$.

It should, however, be pointed out that these equilibrium potential–pH diagrams do not provide any direct kinetic information; the real rate of corrosion and extent of passivation is not evident from a simple examination of the diagrams. Some oxides dissolve only very slowly in certain solutions for kinetic as opposed to thermodynamic reasons. It should also be pointed out that the oxide stoichiometries and the thermodynamic information given in the Pourbaix diagrams are for thick, bulk oxides, which may be quite different from the very thin (nanometer-range) surface oxide films found on passivated metal surfaces. For this reason, it is not surprising that the actual values for $U_p$ and the composition of passive oxide films are sometimes not identical to those found in the Pourbaix diagrams.

*Kinetics*

To understand the kinetics of the reactions involved in passivation, both the anodic metal oxidation and cathodic reactions taking place must be considered. The situation of oxide growth for a metal electrode in an electrolyte is shown schematically in Fig. 3. Although in essence very similar, two slightly different situations are distinguished: Fig. 3a represents the growth of an oxide

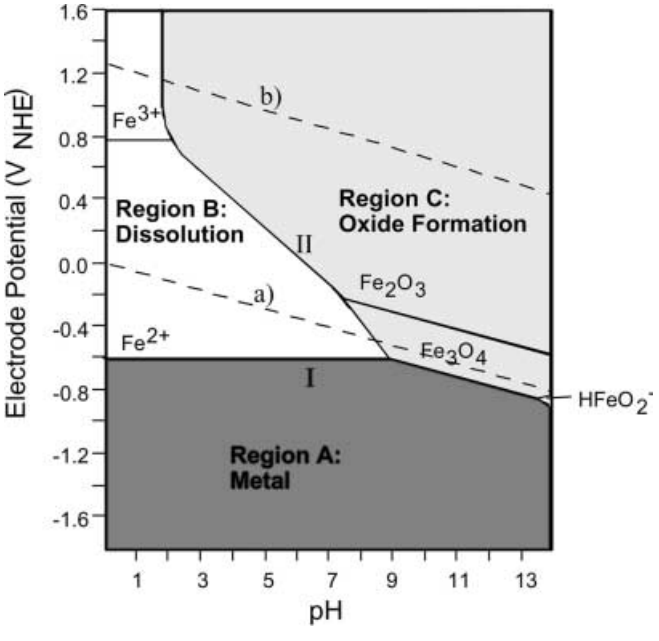


**Fig. 2** Simplified $E$/pH diagram (Pourbaix diagram) for the iron–water system at 25 °C. The diagram is drawn for a concentration of dissolved Fe species of $10^{-6}$ mol/l. The potentials are given versus the normal hydrogen electrode (*NHE*)

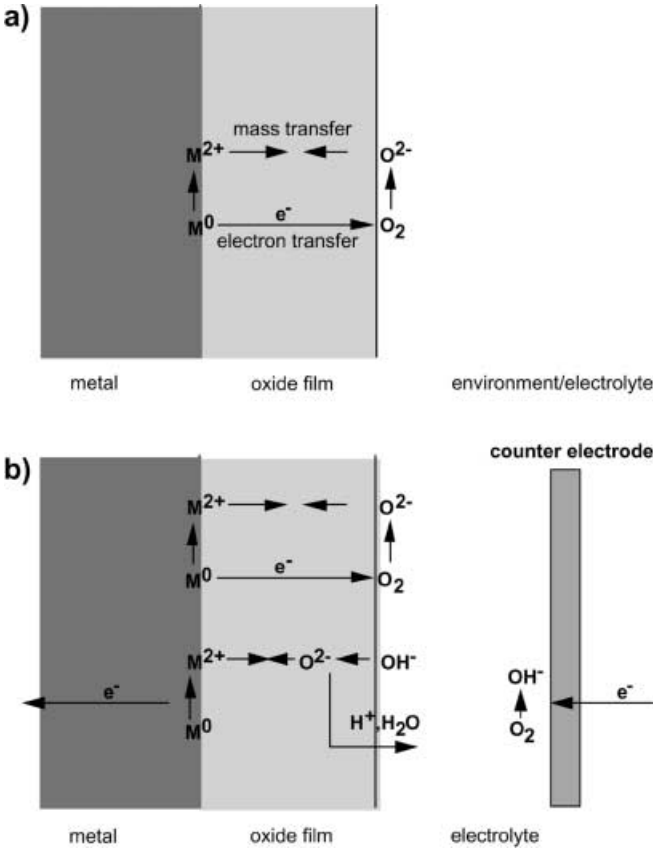


**Fig. 3a, b** Growth of an oxide film on a metal surface. **a** In the absence of an externally applied potential. Metal oxidation ($M \rightarrow M^{2+}$) occurring at the inner interface is coupled with oxygen reduction ($O_2 \rightarrow O^{2-}$) at the outer interface. For film growth one of the ionic species migrates predominantly – mass transfer is coupled with electron transfer through the layer. (This situation also corresponds to high-temperature oxidation). **b** In the presence of an externally applied anodic potential (potentiostat). In addition to the mechanism in **a** film growth can also take place without electron transfer through the film as oxygen reduction happens at the counterelectrode

under open-circuit conditions, i.e., a piece of iron immersed in a passivating solution or exposed to an oxygen-containing environment; Fig. 3b shows the situation under an externally applied voltage in an electrolyte.

In both cases the anodic reaction occurs by oxidation at the metal/oxide interface:

$$M \rightarrow M^{2+} + 2e^{-}. \tag{3}$$

The cathodic reaction is – in this example – the reduction of $O_2$ at the oxide/gas or oxide/electrolyte interface:

$$1/2O_2 + 2e^{-} \rightarrow O^{2-}. \tag{4}$$

At least one of the ionic species has to diffuse or migrate through the oxide and accordingly the layer grows usually either at the inner or at the outer interface (alternatively the transport of ions through the film can be formulated as cation and anion vacancies moving through the lattice of the oxide film) [24, 25, 26]. As the cathodic and anodic reactions are spatially separated by the oxide, electrons also have to be transferred through the layer and, thus, the conductance of the layer is essential to the process. Most oxides are semiconductors owing to a nonequilibrated stoichiometry and, thus, either a negatively or a positively charged species has freedom to migrate through the lattice. The driving force for migration is established by the different electrochemical potentials ($\Delta U$) that exist at the two interfaces of the oxide. In other words, the electrochemical potential at the outer interface is controlled by the dominant red/ox species present in the electrolyte (e.g., $O_2$).

The situation in Fig. 3b is different in that in addition to the mechanism in Fig. 3a, reduction of the red/ox species can occur at the counterelectrode. Thus, electron transfer through the layer may not be needed, as film growth can occur with $OH^{-}$ species present in the electrolyte involving a (field-aided) deprotonation of the film. The driving force is provided by the externally applied voltage, $\Delta U_{\mathrm{appl}}$.

Quantitative descriptions of the kinetics of film formation, i.e., the mechanistic extraction of growth laws for film formation dates back to the work of Cabrera and Mott [27] and Vetter [28]. Essential to their concepts is that at low-to-moderate temperatures and high field strength, $F$ ($F > 10^6$ V/cm), pure diffusion of ionic species is very small compared with field-aided transport.

The distribution of the potential drops across a metal/oxide/electrolyte system is shown schematically in Fig. 4. Models for the oxide growth consider different processes to be rate-determining. The most basic approach assumes that ion transport through the film is controlled by the electric field across the layer. The activation energy for ion or vacancy hopping is lower, the higher the field (so-called high-field mechanism). Cabrera and Mott [27] allocate the rate-determining reaction to the metal/oxide interface, whereas Fehlner and Mott [29] assign the key step to the oxide/environment interface. Refined theories incorporate the buildup of space charges within a nonstoichiometric oxide [30, 31, 32] (nonstoichiometry can be caused by the ions moving through the oxide). However, all these approaches are either represented, or can be approximated, by

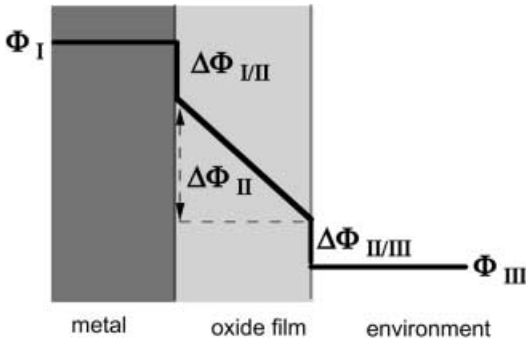


**Fig. 4** Schematic representation of the potential drop across a metal/passive film/environment system. $\Delta\phi_{\mathrm{I/II}}$ and $\Delta\phi_{\mathrm{II/III}}$ represent the interface potential drops and $\Delta\phi_{\mathrm{II}}$ corresponds to the dielectric drop over the oxide layer

$$i = A \exp(\beta F_{\mathrm{ox}}), \tag{5}$$

where $i$ represents the current density, $A$ and $\beta$ are constants, and $F_{\mathrm{ox}}$ is the field strength over the oxide.

The growth according to this equation is self-limiting as $F$ is lowered (at constant voltage) with increasing film thickness, $x$.

$$F(t) = \Delta \mathrm{U}/x(t) \tag{6}$$

This results in the so-called inverse logarithmic growth law for all these models.

$$1/\mathrm{x} = \mathrm{A} - \mathrm{B} \cdot \log(\mathrm{t}) \tag{7}$$

where $x$ is the film thickness, $t$ is the time, and $A$ and $B$ are constants.

A fundamentally different approach postulates that the transport of ions is not rate-determining but that generally the formation of oxide can be described by a process with an activation energy, $W$, that is raised by an amount $\mu x$ during film growth. The approach for the rate law is hence

$$\mathrm{d}x/\mathrm{d}t = \exp[-(W_0 + \mu x)/kT]. \tag{8}$$

Integration leads to the so-called direct logarithmic (activation-energy-controlled) growth law

$$x = K + L \log(1 + Mt), \tag{9}$$

where $K$, $L$, and $M$ are constants.

Several mechanisms have been proposed that could account for the direct logarithmic approach, such as rate limitation by direct electron tunneling from the metal through the oxide [33], by lattice reorganization [29], or by a place exchange mechanism [34, 35, 36, 37, 38].

It should be noted that a variety of other mechanisms of growth have been proposed [39] but they have in common that they result in either the inverse logarithmic or the direct logarithmic growth law. The experimental data obtained up to now for many systems fit both growth laws equally well, and hence it is difficult to distinguish between them.

In practice, the rate laws have been observed for many metals and alloys either oxidized anodically or exposed to oxidizing atmospheres at low to moderate temperatures [40]. Examples are W, Bi, Fe, Ti, Ge, Si, Zr, Sb, InSb, V, Mo, Pt, and Ni [41, 42, 43, 44]; alloys of Al with Mg, Zn, Cu, Si, and Fe [45]; alloys of Nb with Zr, W, Ti, V, and Mo [46]; alloys of V with Nb, Ti, Ta, and Al [47]; and alloys of Ta with Nb, Ti, and Zr [47].

Highly protective layers that are formed by moderate polarization in an electrolyte or in a gaseous environment at ambient temperatures have a thickness typically in the range 1–3 nm. Substantially thicker films can be formed on so-called valve metals (Ti, Ta, Zr,...), which allow the application of comparably high anodizing potentials (high electric fields) before dielectric breakdown occurs.

In most practical cases (and moderate voltages), a high-field growth law can control film growth, say up to only a maximum of 10 nm as at this thickness the field strength effects become even less important than film growth due to diffusion of vacancies or ions. At elevated temperatures, scales can grow much thicker in, for example, water, air, oxygen, or other more aggressive gases containing sulfur or chlorine. Mechanistically, elevated temperatures promote ionic diffusion and thus oxide formation can proceed to a much greater extent than at low temperatures. In accordance with diffusion being the dominant process, the most common growth law observed at higher temperatures is the so-called parabolic rate law [48]:

$$x^2 = k_p t + C, \tag{10}$$

where $k_p$ is the parabolic rate constant.

As mentioned, whether a high field or a thermal diffusion process is rate-controlling, either oxygen (anions) or cations or both can be the dominant mobile species to move through the layer (Fig. 5a). Investigations using markers often show mixed control, i.e., both cations and anions move, such as for oxides on Al, Be, Nb, Ta, Ti, V, and W with cation-transfer numbers ranging from 0.3 to 0.7. Important exceptions in this respect are Si, Hf, and Zr, which show oxide growth almost exclusively by anion transport (with anion-transfer numbers above 0.9) [49, 50, 51].

Another kinetic phenomenon that is frequently encountered with passive films is so-called "aging". It addresses the experimental finding that passive film properties, such as composition, structure, degree of hydration, and ionic or electronic conductivity, can considerably alter with time. Although these changes are sometimes of great practical significance, as they usually improve the corrosion resistance of materials, they have been much less investigated – mostly because of the complexity of the mechanisms and the extended time scales involved.

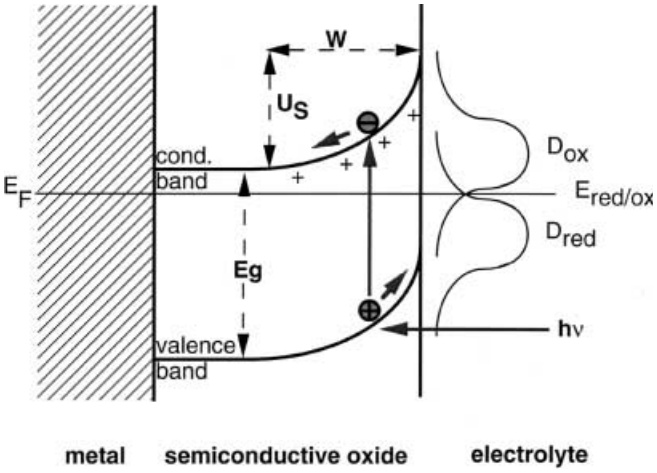


**Fig. 5** Energetic situation at an n-type semiconductor passive film/electrolyte interface with the formation of a Schottky barrier (height, $U_s$, width, $W$) and the energetic distribution of oxidized ($D_{ox}$) and reduced ($D_{red}$) species in the electrolyte. The photocurrent generation (*gray*), i.e., electron–hole pair formation by the interaction with light ($h\nu > E_g$) is also indicated

## Passive film characteristics

### *Chemical composition*

The nature of passive oxide films on many technologically important metals and alloys has been the subject of investigation for many years. Ex situ surface analytical techniques such as X-ray photoelectron spectroscopy (XPS), Auger electron spectroscopy, and secondary ion mass spectrometry (SIMS) provide useful information on the chemical composition and thickness of the films. Good agreement exists regarding a qualitative description of the chemistry of passive films on many metals; however, owing to either different experimental approaches or to data analysis, slightly different views can be found on the more detailed nature of the different films. Generally, it is important to note that, once formed, the passive film should not be considered as a rigid layer, but instead as a system in dynamic equilibrium between film dissolution and growth. In other words, the passive film can adjust its composition and thickness to changing environmental factors. Principally, the chemical composition and the thickness of electrochemically formed passive films depend (apart from the base metal) on the passivation potential, time, electrolyte composition, and temperature, i.e., on all passivation parameters, and hence a detailed treatment is beyond the scope of this work. For further relevant literature the reader is referred to Refs. [52, 53, 54, 55, 56,

57, 58, 59, 60, 61, 62, 63, 64, 65, 66, 67] and references therein.

### *Structure*

Several research groups have tackled the question of the structure of passive films. Methods used to investigate the structure include X-ray scattering, diffraction, and Mössbauer spectroscopy. For thick anodic oxide films or thick oxide films grown at elevated temperatures, the structure can be accessed by X-ray diffraction techniques; however, for thin passive films formed at low-to-moderate temperatures, the thickness of the films is usually less than 10 nm, and hence it is experimentally difficult to investigate the structure by traditional X-ray diffraction. Another question often asked is whether the structure of a thin, mostly hydrated passive film formed under electrochemical conditions may change as it is removed from the condition under which it was formed. Therefore, new in situ techniques (scanning tunneling microscopy, STM, X-ray scattering using synchrotron radiation, and extended X-ray absorption fine structure, EXAFS) have lately been used to study the structure of thin oxide films. In the case of the passive film on Fe, for instance, it was shown with in situ STM [68] as well as with in situ X-ray scattering [69] that the passive film has a crystalline structure. Up to now, however, these investigations have been extended to only a few metals, and hence the question of the structure of passive films remains to be investigated further.

### *Electronic properties*

As already outlined, electron transfer through the passive film can also be crucial for passivation and thus for the corrosion behavior of a metal. Electronically, oxide films can show metallic behavior, such as $IrO_2$, $RuO_2$, $PbO_2$, semiconductor behavior, such as oxides on Ti, Fe, Sn, Sb, Nb, Bi, W, Cu, Ni, and Cr, or can be insulators, such as the oxides on Ta, Zr, Hf, and Al (see also Table 1). As many anodically formed passive films are of a semiconductive nature [81, 85, 88, 89, 90, 91, 92, 93, 94, 95, 96, 97, 98, 99], the electronic properties principally can be investigated with techniques borrowed from ideal semiconductor electrochemistry (most typically photoelectrochemistry and capacitance measurements of the Mott–Schottky type) [100].

The energetic situation in terms of a band model for a metal/semiconductor/electrolyte interface is illustrated in Fig. 5. If the passive film behaves like an ideal semiconductor, a Schottky barrier is present at the semiconductor electrolyte interface. The barrier can be described, as indicated in Fig. 5, in terms of a height, $U_s$, and a width, $W$:

$$W = \left| \frac{2\varepsilon\varepsilon_0}{qN} \left( U_S - \frac{kT}{q} \right) \right|^{0.5} \tag{11}$$

where $q$ is the charge of an electron, $\epsilon_0$ the permittivity of a vacuum, $k$ the Boltzmann constant, $T$ the temperature, $\epsilon$ the dielectric constant, and $N$ the doping concentration of the semiconductor.

The barrier height is either $U_s = U_{appl} - U_{fb}$ in the case of anodic polarization or $U_s = E_{red/ox} - U_{fb}$ if the semiconductor is immersed in an electrolyte without external polarization ($E_{red/ox}$ represents the red/ox potential of the electrolyte); $U_{fb}$, the flat-band potential is the potential at which $U_s = 0$, i.e., the bands in the semiconductor are "flat". $W$ corresponds to the depth of the space charge layer generated by ionized doping species.

As a consequence, the space charge capacitance, $C_{sc}$, measured using, for example, alternating current impedance or pulse techniques, can be obtained. By employing a parallel plate condensor model, $C_{sc}$ is

**Table 1** Electronic properties of oxide films on some metals and alloys. Band-gap energy, $E_g$, doping concentration, $N$, dielectric constant, $\epsilon_{ox}$, n-type conductor, $n$, p-type conductor, $p$, insulator, $i$

| Metal/alloy | Oxide | | | | Ref. |
|---|---|---|---|---|---|
| | $E_g$ (eV) | $N$ ($cm^{-3}$) | $\epsilon_{ox}$ | Conduction type | |
| Al | 4.5–9 | – | 7–20 | i | [70] |
| Al/Cr | – | – | – | n | [71] |
| Cr | 2.5–3.5 | $10^{20}$ | $30 \pm 20$ | p(n)? | [72, 73, 74, 75, 76, 77] |
| Cu | 0.6–1.8 | ? | 7–18 | p | [70, 78] |
| Fe | 1.8–2.2 | $10^{20}$ | 10–35 | n | [79, 80, 81] |
| Fe/Cr | 1.9–2.1 | $10^{20}$–$10^{21}$ | 10–30 | n | [82] |
| Fe/Cr/Ni (AISI304) | 1.9–2.3 | $10^{20}$–$10^{21}$ | 10–30 | n | [83, 84, 85, 86] |
| Fe/Cr/Ni/Mo (SMO254, DIN1.4529) | 2.3–2.8 | $10^{21}$ | 10–30 | n | [85, 86, 87] |
| Fe/Ni ($x_{Ni} < 40\%$) | 1.9 | $10^{20}$ | 10–35 | n | [82] |
| Ni | 2.2–3.7 | $10^{20}$ | 30 | p(n) | [72, 81, 88] |
| Sn | 3.5–3.7 | $10^{19}$–$10^{20}$ | ? | n | [78] |
| Ti | 3.2–3.8 | $10^{20}$ | 7–114 | n | [70] |
| W | 2.7–3.1 | $10^{17}$–$10^{18}$ | 23–57 | n | [78] |
| Zn | 3.2 | $10^{18}$ | 8.5 | n | [78] |
| Zr | 4.6–8 | – | 12–31 | i, n | [70, 78] |

interlinked with $W$ by $C_{sc} = \epsilon\epsilon_0/W$ and thus from the so-called Mott–Schottky plots ($C^{-2}$ versus $U_{appl}$), $U_{fb}$ and the doping concentration, $N$, can be obtained (assuming $\epsilon_{ox}$ is known) [100].

Another type of experiment to characterize the electronic properties is photocurrent measurement: If light of sufficient energy ($h\nu > E_g$) hits a semiconductor, electrons from the valence band can be excited to the conduction band. The resulting electron–hole pair is separated in the field of the Schottky barrier and, therefore, a photocurrent is generated. For thin semiconductive layers the photocurrent, $I_{ph}$, can be approximated by [101, 102]:

$$I_{ph} = q\Phi\alpha W, \tag{12}$$

where $\Phi$ is the incident light intensity and $\alpha$ is the optical absorption coefficient of the film, given by [103]

$$\alpha = A\frac{(h\nu - E_g)^n}{h\nu}, \tag{13}$$

where $A$ is a constant depending on the electronic structure of the material, $n$ is a constant depending on the nature of the electron transition ($n = 0.5$ for direct and $n = 2$ for indirect, or amorphous, transitions), and $h\nu$ is the energy of the light.

Thus, from $(I_{ph}–h\nu)^{1/n}$ versus $h\nu$ plots (measured at a constant potential) the band-gap energy can be determined. By using Eqs. (11) and (12) one can obtain the flat-band potential from $I_{ph}$ versus $U_{appl}$ plots. Additionally, from the sign of the photocurrent, the conduction type of the semiconductor can be determined.

Another consequence of the presence of a semiconductor-type Schottky barrier is that electron-transfer reactions with defined red/ox couples in the electrolyte (e.g. $Fe(CN)_6^{4-}/Fe(CN)_6^{3-}$) show asymmetrical behavior regarding anodic and cathodic reactions – apparent, for example, in $I$–$U$ curves. In accord with the Gerischer model [104] this asymmetry stems from the fact that, for example, for an n-type semiconductor, electron transfer from the conduction band to the $D_{ox}$ states in the electrolyte depends on the barrier height $U_s$ that can be reduced by a cathodic $U_{appl}$, while for the reverse reaction (electron transfer from $D_{red}$ to the conduction band) the barrier is potential-independent (cf. Fig. 5).

It should be pointed out that passive films often show considerable deviations from ideal semiconductor behavior. Passive films, compared with bulk semiconductors, frequently possess a small thickness (only a few nanometers for nonvalve metals), have a nonideal crystalline structure (amorphous or highly defective), show mobile doping species, and often exhibit doping levels close to degeneracy [100].

The small thickness limits the extension of the space charge layer. Usually, a high field strength is obtained in the passive film already at potentials relatively near the flat-band potential. Further, for nanometer-range thicknesses it is questionable whether the presence of a long-range order and, hence, an ideal band structure can be established.

Additionally, the highly defective nature of many passive films contributes to a nonideal band structure. The differences in the distribution of the density of states, $N(E)$, in an ideal and in a defective semiconductor are illustrated in Fig. 6. For a nonideal semiconductor the concept of a band gap ($E_g$) is replaced by a mobility gap ($E_{mg}$) accompanied with a tail of localized states into the gap [105, 106].

Furthermore, deep donor bands or a high number of surface states (dangling bonds), can be present within the energy range of the band gap. All these additional states can influence the ion and charge transfer within the film and, thus, affect photoelectrochemical, capacitance, and charge-transfer measurements. This leads to significant deviations in Mott–Schottky plots (nonlinearity, frequency dispersion); photoelectrochemical experiments exhibit sub-band-gap responses (Urbach tail [88]) and frequently a potential dependence of the photocurrent may be obtained that instead of fitting $I_{ph} \propto U_{appl}{}^{0.5}$ rather fits $I_{ph} \propto \exp(U_{appl})$ [86].

In spite of these complications, valuable information on the electronic properties of many oxide films has been obtained. A brief overview and reference to further information is provided in Table 1.

## Passive film protectiveness

The protective quality of a passive film is determined by the ion transfer through the film as well as by the stability of the film against dissolution. Using polarization curves, the "protectiveness" of a passive film in a certain environment can be estimated from the passive current density, $i_{pass}$ (Fig. 1). It is clear that a variety of factors can influence ion transport through the film, such as the film's chemical composition, structure, number of grain boundaries, and the extent of flaws and pores. The dissolution of passive oxide films can occur either chemically or electrochemically. The latter case takes place if an oxidized or reduced component of the passive film is more soluble in the electrolyte than the original component.

A variety of approaches have been taken to establish a framework that fundamentally explains the

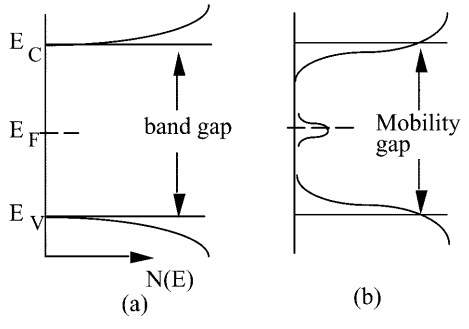


**Fig. 6** Density-of-states distribution in **a** an ideal and **b** an amorphous or defective semiconductor after Ref. [105]

protectiveness and stability of passive films. While for passive films formed on pure metals mainly structural and chemical information can lead to a straightforward explanation, the situation is more complex for alloys. In this case, approaches have, for instance, been based on percolation arguments [107, 108], structural arguments [109], ion/defect mobility [25, 26], and charge distribution [110, 111].

To illustrate some of the different views let us consider passive films grown on Fe–Cr alloys. The percolation argument is based on the idea that with increasing Cr content in the alloy an insoluble, interlinked chromium oxide network can form within the passive film (the iron compounds are considered as soluble and nonprotective). A continuous (protective) Cr network, however, is only possible once a critical Cr content in the alloy (corresponding to the percolation threshold) is present. The model seems to hold for specific environmental conditions. However, as the threshold composition for the high stability of the oxide film is strongly influenced by solution chemistry and is different for different dissolution reactions [112], it must be argued that a model cannot be based on purely geometrical considerations but has, in addition, to consider the dissolution chemistry.

Other authors have correlated the improved corrosion resistance with increasing Cr content in the alloy with the increasing tendency of the oxide to become more disordered with higher Cr content [109]. This would then suggest that an amorphous oxide film is more protective than a crystalline one, owing to bond and structural flexibility in amorphous films.

Another approach to explain the stability of oxide films is mainly based on the work of Sakashita and Sato [110], who assign a key role to the ion selectivity within films. According to these authors, a bipolar passive film consists of an anion-selective layer on the metal side of the passive film and a cation-selective layer on the solution side. As a result the ionic current in the anodic direction is retarded. An anodic voltage imposed will cause dehydration of the deposit layer with hydrogen ions moving through the cation-selective layer toward the solution and with the movement of metal ions retarded in the anion-selective inner layer. Eventually a dehydrated protective oxide film is formed on the metal surface. In a similar manner, Clayton and coworkers [111, 113] explain the passivity of stainless steel to be due to the formation of a bipolar passive film through incorporation of $CrO_4^{2-}$ anions in the outer layer of the passive film. They based their modeling on a XPS investigation of the passive films, where they found $CrO_4^{2-}$ anions in the outer layer of the film and, as the bipolar passivity model predicts, in the inner part of the film a layer of $Cr_2O_3$.

All the previous mechanisms seem to be able to explain the passivity of some alloy/electrolyte systems. Still no comprehensive and conclusive model exists. This may be ascribed to the fact that the composition and structure of the passive films strongly depend on the passivation parameters, and thus a comparison of different results is often difficult. Therefore, more information on the chemistry, structure, and protectiveness of passive films is still needed to create a conclusive and "universal" approach to the stability of passive films.

## Breakdown of passivity

### Localized corrosion

The passive state of a metal can, under certain circumstances, be prone to localized instabilities. The most extensively investigated is that of localized dissolution events on oxide passivated surfaces [114, 115, 116, 117, 118, 119, 120, 121, 122, 123, 124, 125, 126, 127]. The essence of localized corrosion is that distinct anodic sites on the surface can be identified where the active metal dissolution reaction (e.g., $Fe \rightarrow Fe^{2+} + 2e^-$) dominates, surrounded by a passivated cathodic zone where the reduction reaction takes place (e.g., $2H^+ + 2e^- \rightarrow H_2$). The result is the formation of an active pit in the metal, as illustrated schematically in Fig. 7.

Pitting occurs with many metals in halide-containing solutions. Typical examples of metallic materials prone to pitting corrosion are Fe, stainless steels, and Al. The process is autocatalytic, i.e., by initial dissolution conditions are established which further stimulate dissolution: inside the pit the metal dissolves. The $M^{2+}$ species form an aquo complex:

$$M^{2+} + 6H_2O \rightarrow M(H_2O)_6^{2+}, \tag{14}$$

To maintain charge neutrality additional halide ions ($Cl^-$ in our example) have to migrate inside the pit, thus

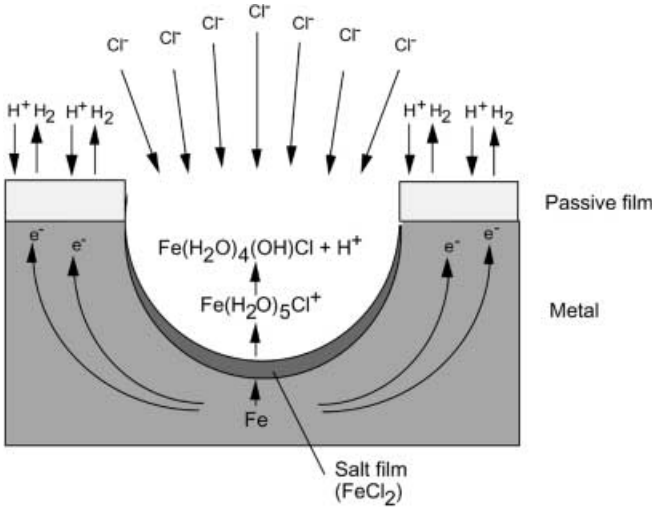


**Fig. 7** Schematic cross section through an actively growing pit. Metal oxidation occurs at the pit base and the corresponding reduction reaction (e.g., $H_2$ evolution in acidic solutions or $O_2$ reduction in aerated neutral solutions) on the passive film surrounding the pit. Acidification and an increase in the halogen ion concentration (owing to migration) within the pit additionally accelerate dissolution

increasing the local chloride concentration and a chloro complex is formed.

$$M(H_2O)_6^{2+} + Cl^- \rightarrow M(H_2O)_5Cl^+ + H_2$$
$$\leftrightarrow M(H_2O)_4(OH)Cl + H^+ \quad (15)$$

For many metals the equilibrium lies strongly to the right-hand side. Thus, within the pit the chloride concentration and the $H^+$ concentration both increase, further accelerating metal dissolution.

Generally speaking, one can distinguish the following two stages of pitting: pit initiation and pit growth. The reasons for the initiation of pits at distinct surface locations are manifold and can either be deterministic or stochastic in nature. They can be ascribed to bulk metal inhomogeneities (inclusions, precipitates, grain boundaries, dislocations, etc.) or to properties of the passive film (thermally induced stochastic film rupture, electrostriction, local composition, or structure variations). Initiation mechanisms assigning the key role to the passive film involve $Cl^-$ penetration, local film thinning, and vacancy condensation; mechanisms focusing on the bulk metal ascribe the key role to preferential dissolution at inhomogeneities.

In an electrochemical polarization experiment of a passive system the onset of localized dissolution can be detected by a steep current increase at a very distinct anodic potential (the pitting potential, $U_{pit}$) – see Fig. 8. This increase occurs far below either transpassive dissolution or the occurrence of oxygen evolution ($OH^- \rightarrow O_2$).

In the potential range anodic to $U_{pit}$ stable pit growth occurs. In general, $U_{pit}$ is shifted to lower anodic potentials with increasing temperature, increasing $Cl^-$ concentration, and decreasing pH and is dependent on the presence of other anions in the electrolyte.

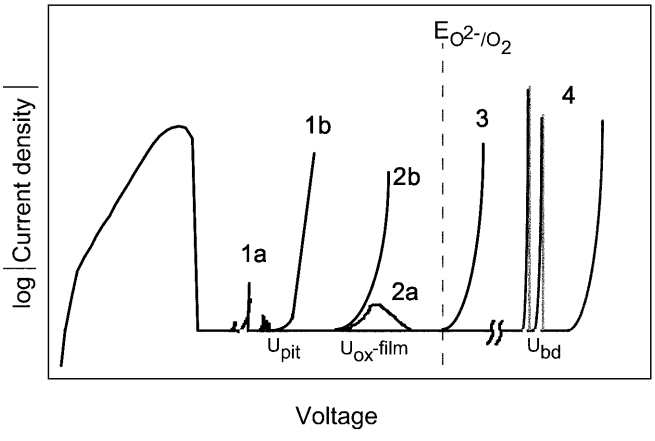


**Fig. 8** Polarization curve of a passive metal showing schematically typical passivity breakdown possibilities: *1* localized corrosion in the presence of an "aggressive" anion, *1a* current transients owing to metastable pitting, *1b* stable pit growth at $U_{pit}$; *2* passivity breakdown owing to oxidative film dissolution, *2a* if secondary passivation occurs (e.g., in mixed oxides with one stable compound), *2b* in the absence of secondary passivation; *3* current increase owing to oxygen evolution; *4* dielectric breakdown (typically at comparably high applied voltages)

From an electrochemical viewpoint stable pit growth is maintained as long as the local environment within the pit keeps the pit under active conditions. Thus, the effective potential at the pit base must be less anodic than the passivation potential ($U_p$) of the metal in the pit electrolyte. This may require the presence of voltage drop (*IR* drop) elements. In this respect the most important factor appears to be the formation of a salt film at the pit base. (The salt film forms because the solubility limit of, for example, $FeCl_2$ is exceeded in the vicinity of the dissolving surface in the highly $Cl^-$ concentrated electrolyte).

In the potential range cathodic to $U_{pit}$, one frequently observes so-called metastable pitting. A number of pit growth events are initiated, but the pits immediately repassivate (an oxide film is formed in the pit) because the conditions within the pit are such that no stable pit growth can be maintained. This results in a polarization curve with strong current oscillations at $U < U_{pit}$.

In all cases of localized corrosion, the ratio of the cathodic to the anodic area plays a major role in the localized dissolution rate. A large cathodic area provides high cathodic currents and, owing to electroneutrality requirements, the small anodic area must provide a high anodic current; hence, the local current density, i.e., local corrosion rate, becomes higher with a larger cathode/anode ratio.

Recently, the phenomenon of localized dissolution has also attracted a great deal of interest in the field of semiconductor technology. This is due to the discovery of visible light emission from porous Si [128] which is formed by an electrochemical treatment of a Si surface in a HF-containing electrolyte [129]. It is interesting to note that the formation process is in many respects similar to pitting of metals [127] and that preferential triggering of the formation process at defects can be exploited to form highly defined localized dissolution [130].

## Electric, dielectric breakdown

Electric breakdown of an insulating region, such as an insulating oxide layer or the depletion region in a semiconductive layer, occurs if extra charge carriers are generated either by tunneling (Zener breakdown) or by collision (avalanche breakdown). In other words, if a sufficient electric field is applied to an oxide film, dielectric breakdown will take place. This is apparent in *I–U* curves by a current increase, at a distinct voltage $U_{bd}$ [78, 131, 132, 133, 134], or by current or potential fluctuations (Fig. 8). Such breakdown events can also become apparent by sparking or acoustically (crackling noise). For example, Wood and Pearson [135] discuss anodic breakdown of oxide films on the valve metals Nb, Ta, Zr, Hf, Al, Ti, W, Mo, and V. It is of interest to note that according to these authors Ti and W, whose oxide

films are semiconductors, did not break down, but turned into conductors, leading to oxygen evolution. Generally, breakdown on valve metals results in thickening of films at locations where the breakdown occurred, and thus pinches itself off. Therefore, the breakdown spot may meander over the surface. Wood and Pearson concluded that avalanche breakdown was observed at sites where the electrons initiating the avalanche are supplied by the electrolyte.

Particularly breakdown in electrolytes under cathodic polarization may be strongly influenced by cation in-diffusion and accompanying alterations in the electronic structure of the oxide (e.g., incorporation of additional states within the band gap). The most likely mobile species are protons. For example, Dyer and Leach [136] examined oxidized titanium and niobium and found that hydrogen enters the film under cathodic bias in non-negligible amounts. $TiO_2$, for example, can to a large extent (up to 85%) be converted to TiOOH, as concluded from observations of the change in the index of refraction. Thus cation in-diffusion into passivating films can be substantial under cathodic bias. Hydrogen ingress into Ti oxide layers by cathodic polarization has recently also been studied by in situ neutron reflectometry [137].

In general, current passage through oxide layers when the metals are biased cathodically is common on valve metals, for example, zirconium, tantalum, and aluminium, but also oxides on silicon can show significant cathodic currents. Schmidt [138, 139] suggests that these cathodic currents are related to the in-diffusion of protons, since with tantalum and silicon it was found that if an anhydrous electrolyte is used, there is no cathodic current. Vermilyea [140] and others [141] showed that the cathodic currents are laterally inhomogeneous and correspond to flaws in the oxide.

The effect of mobile ions on the current passage has been studied particularly well in the case of silicon, where also the band model and the defect structure are well known. Specifically, the effect of mobile $Na^+$ in $SiO_2$ on electron flow into and through the oxide has been investigated in depth, as the presence of $Na^+$ in $SiO_2$ can have a drastic detrimental effect on the performance of metal oxide semiconductor devices [142, 143, 144, 145].

## Anodic, cathodic, and chemical film dissolution

The stability of passive films can be limited by anodic or cathodic red/ox processes. In essence, whenever the thermodynamic situation is such that under the given environmental conditions ($U$, pH) a reductive or oxidative reaction of the oxide is favored (see Pourbaix diagrams) and the reduced or oxidized species is soluble in the electrolyte, depassivation may occur. Additionally, also plain chemical dissolution by complexing agents may take place [146]. Examples are the action of fluorides, for example, on dissolution of $TiO_2$ or $SiO_2$ by the formation of fluoro complexes. Therefore, for a complete thermodynamic description of the stability of oxide films in a given solution the effect of complexing species present in the solution has to be considered and corresponding Pourbaix diagrams have to be used.

In general, electrochemical or chemical film dissolution can be favored at inhomogeneities of the film, such as dislocations or edges of oxide islands, and thus show a high degree of nonuniformity.

The most prominent examples of red/ox reactions of oxide films (in the context of passivity of construction metals and alloys) are the oxidative dissolution of $Cr_2O_3$ to $CrO_4^{2-}$, the reduction of $Fe_2O_3$ to soluble $Fe^{2+}$ or to $Fe^0$, the reduction of NiOOH to NiO, and the reduction of CuO into $Cu_2O$.

In the following, we briefly discuss the red/ox mechanisms of the first two examples.

### *$Cr_2O_3$ and the passive film on Cr*

Sufficient anodic polarization of $Cr_2O_3$ or passive films on Cr leads to an oxidation of the $Cr^{3+}$ to the soluble $Cr^{6+}$ species ($CrO_4^{2-}$, $Cr_2O_7^{2-}$) [76, 147, 148, 149, 150, 151, 152]. In accordance with the thermodynamical prediction, the reactions sets in at potentials below oxygen evolution from the aqueous electrolyte and in polarization curves the oxidation reaction manifests itself through a current increase at the corresponding potentials (Fig. 8). For pure Cr a steep current increase is observed which is accompanied by "transpassive" dissolution of the sample. In mixed oxide films where the second oxide is stable under these electrochemical conditions, the $Cr_2O_3$ part may selectively be oxidized, leading only to a peak in the polarization curve. This situation is typically encountered with Fe–Cr alloys, where passivation can be maintained by the presence of the Fe oxides. Some of the hexavalent Cr may remain trapped in the film.

### *$Fe_2O_3$ and the passive film on Fe*

Under reductive conditions, the $Fe^{3+}$ species in the passive film on iron or $Fe_2O_3$ layers can be reduced to $Fe^{2+}$ (or $Fe^0$) [153, 154, 155, 156]. The consequences of the reduction depend strongly on the electrolyte composition. In borate buffer (pH 8.4), reduction leads to the complete dissolution of the Fe oxide films, with a current efficiency of 100%. In acidic solution, dissolution efficiencies much greater than 100% are observed, owing to chemical dissolution of the iron oxides accompanying reductive dissolution. In alkaline solution, no dissolution takes place, but, instead, the Fe oxide films are converted into a lower-valent oxide/hydroxide film during the reduction. For phosphate buffer solutions in the neutral and alkaline range reduction can lead to metallic iron, Fe(0).

## Aspects of passivity of some important metals and alloys

### Iron

*Active/passive transition*

Most investigations on the passivity of pure Fe have been carried out in alkaline (e.g., 0.1 M NaOH) or in near-neutral borate buffer (pH 8.4) solutions. Fe can also be passivated in 1 M $H_2SO_4$, but in this acidic solution passivation is accompanied with strong dissolution. Passivation in 1 M $H_2SO_4$ proceeds through the formation of a thick, porous Fe sulfate layer on the metal surface [157]. In the polarization curves, a region of high limiting current density follows the active region, the current being limited by the solubility of the Fe sulfate layer (hence, this current density depends on the hydrodynamic conditions). At sufficiently high anodic potentials (stability region of $Fe^{3+}$ oxides), the true current density in the pores of the salt layer exceeds the critical current density for passivation, and hence the formation of a stable Fe oxide film in the pores and below the salt layer can take place. After oxide passivation is complete, the remaining Fe sulfate layer dissolves.

The critical current density for passivation is strongly pH-dependent, as shown in Fig. 9. With increasing pH, the values of the passivation potential are shifted in the negative direction. The passivation mechanism in all solutions is considered to involve a precipitation of Fe(II) salts [e.g., $Fe(OH)_2$] in the region of the active/passive transition, followed by the formation of a Fe oxide layer in the passive range. In alkaline solutions (pH > 11.5) iron will be spontaneously passive under most conditions.

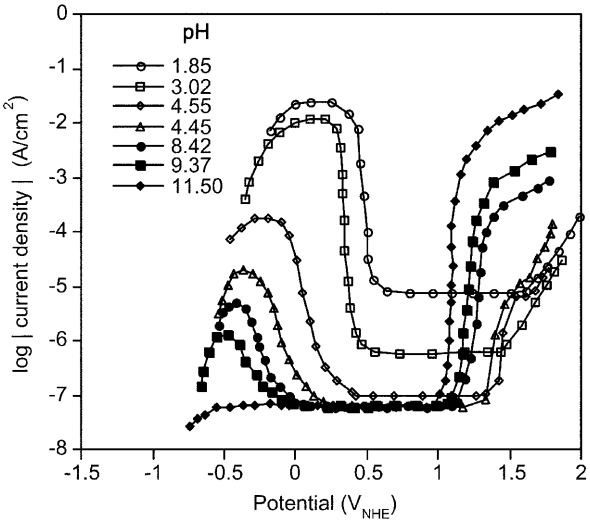


**Fig. 9** Anodic potentiostatic polarization curves for iron in 0.15 M $Na_3PO_4$ solutions of different pH (after N. Sato in Ref. [12], p. 29)

*Chemistry and structure of the film*

Even though it is generally agreed that passivation of iron is caused by the formation of a 3D oxide phase on the metal surface, controversy exists on the details of this phase. One classical disagreement concerning the nature of the passive film on Fe is the question of a single-layer or a multiple-layer structure. Earlier studies of the passive film on Fe often describe the film to be a double-layer structure consisting of an outer maghemite ($\gamma$-$Fe_2O_3$) and an inner magnetite ($Fe_3O_4$) layer [158, 159, 160, 161, 162, 163]. This interpretation has often been based on the finding of two reduction waves in galvanostatic reduction experiments. Other investigators using similar approaches, however, concluded that the passive film consists of a single-layer $Fe_2O_3$ similar structure [91, 164, 165, 166]. In these studies a different reduction mechanism for the passive film was assumed, and hence similar results led to a fundamentally different interpretation. As has been discussed in Ref. [153], the finding of two reduction steps during galvanostatic reduction experiments of passive iron (e.g., using ellipsometry or SIMS to study the passive film thickness as a function of the charge) does not necessarily mean that a two-layer structure was initially present on the surface. The results nevertheless do not exclude the possibility that native passive films may be more complex than single-layer $Fe_2O_3$ films. In this context, recent surface-enhanced Raman investigations indicate a more complex reduction behavior of the passive film than expected for a homogeneous single-layer film [167].

Another approach for a two-layered structure of the passive film on iron describes the film to consist of an inner oxide film and an outer hydrated film [168, 169]. Generally, the degree of hydration in the passive film has been discussed to vary between a strongly hydrated and an anhydrous film (see Refs. [170, 171] and references therein). Today there seems to be rather wide agreement that in most cases the incorporation of hydrogen in the oxide layer is limited to the surface of the passive film, and hence is present as a deposit hydroxide layer above the passivating anhydrous barrier layer [170, 171]. It has recently been shown that the presence or absence of a FeOOH-type deposit strongly depends on the experimental conditions during passivation, i.e., on the amount of dissolved $Fe^{2+}$ in the electrolyte in the vicinity of the electrode surface [170].

Apart from the question of the homogeneous/layered construct of the passive film on Fe, a lot of effort has been devoted to the elucidation of the crystal structure of the film. The earliest studies used a stripping method to isolate the passive film from its substrate and then applied diffraction methods to determine the crystal structure, which was concluded to resemble $\gamma$-$Fe_2O_3$ or $Fe_3O_4$ [172, 173, 174]. Later other authors concluded from in situ Mössbauer spectroscopy [175] or surface-enhanced Raman data [176] that the passive film was amorphous in nature. In situ X-ray absorption near-edge spectroscopy and EXAFS studies, however, suggest

that the film has a spinel structure [177, 178]. Confirmation for the crystalline structure of the passive film has recently been given by in situ STM and in situ surface X-ray diffraction techniques [68, 69, 171]. The in situ surface X-ray diffraction studies show the passive film to consist of a new spinel phase [69, 171], with a decreasing amount of $Fe^{2+}$ in the film with increasing passivation potential [179, 180].

### *Electronic properties of the passive film*

The electronic properties of the passive film on iron were studied over the past decades in numerous investigations using capacitance and photocurrent techniques as well as measurements of electron-transfer reactions with defined red/ox couples added to the electrolyte.

From capacitance measurements [79, 89, 91, 92, 181, 182, 183, 184, 185, 186, 187, 188, 189, 190, 191, 192, 193, 194, 195, 196, 197, 198, 199] it is clear that the oxide film behaves as a highly doped n-type semiconductor. Generally, the capacitive behavior shows three different regions:

- At low potentials, ($U$–$U_{fb}$) a Mott–Schottky-type of behavior is observed.
- At higher potentials, a deviation or a plateau is found, which has been interpreted as dielectric behavior or the presence of a deep donor species.
- At even higher potentials, the capacitance increases with potential; this has been attributed, for example, to the contribution of the valence band.

Typically the capacitance behavior shows a significant frequency dispersion. This finding has been ascribed to the contribution of deep donor levels [200] that are located 0.9 eV below the conduction band, as a frequency-dependent dielectricity constant [201], as concentration gradients in the passive film, or as a capacitance contribution of surface states [92].

Studies on electron-transfer reactions [79, 89, 181, 193] show a valence band conduction mechanism at low potentials. At higher potentials, charge transfer takes place by a donor term 0.6 eV above the valence band [89] or, alternatively, by resonance tunneling [202].

The presence of two donor levels in the passive film has been attributed by Stimming [203] to the octahedral or tetrahedral sites in the spinel structure. The donors are $Fe^{2+}$ ions which occupy part of the octahedral and tetrahedral sites. This implies that the stoichiometry of the film differs slightly from $\gamma$-$Fe_2O_3$ (all $Fe^{3+}$ sites are occupied). Gerischer [95], on the other hand, attributes the deep donor level to a Fe3$d$/O2$p$ hybrid orbital, which is situated below the conduction band. (The conduction band is assumed to consist of a Fe3$d$/O2$p$ hybrid orbital with lesser participation of O2$p$ [203] than the deep donor state.)

Different authors have investigated the passive film on Fe with photocurrent spectroscopy [80, 81, 182, 193, 205]. In general, the photocurrent spectra can be interpreted using an ideal crystalline semiconductor approach, which yields an indirect band gap of 1.9 eV. In an extensive investigation of iron in pH 8.4 borate buffer it was found that the band-gap energy is potential-dependent in the potential region 0–300 mV versus the saturated calomel electrode (SCE), followed by a nearly constant value of 1.9 eV at higher potentials. It was further observed by Gärtner that the photocurrent at a constant wavelength shows an exponential potential dependence that cannot be described using the classical model and the behavior $i_{ph} \propto U_{appl}^{0.5}$ was predicted. Therefore, the potential dependence of the photocurrent was interpreted in terms of a field-aided escape from deep states according to a Poole–Frenkel approach [88]. Above a potential of 700 mV, the photocurrent started to decrease with potential, which may be ascribed to the contribution of surface or localized states in the electron–hole recombination kinetics.

The evaluation of the photoresponse is additionally complicated by the fact that the photocurrent transients show nonideal behavior. An explanation was given by Abrantes et al. [199], who describe the transient kinetics by OH radicals, generated at adsorbed $OH^-$ reacting with $h^+$ at $Fe^{3+}$ sites of the passive film.

In summary, some controversy exists on the detailed nature of the passive film on Fe, even though it represents by far the most extensively studied passive metal system. Since the characteristics of the film depend on many passivation parameters, at least some of the controversy can be due to different experimental conditions. Nevertheless, emerging new techniques to study the chemistry and structure of passive films in situ have certainly elucidated the matter in great detail. An excellent review on the historical development of the understanding of the nature of the passive film on Fe has been given recently in Ref. [171].

## Fe–Cr alloys and stainless steels

### *Active/passive transition*

The pH region of stable passivity is strongly enlarged by alloying Cr into Fe. The remarkable changes in the corrosion behavior of Fe–Cr alloys at a critical Cr concentration were systematically studied by Monnartz in 1911 [7]. Since these early studies, the existence and origin of critical threshold values for the Cr concentration in Fe–Cr alloys has often been discussed. In a study of the corrosion behavior of Fe–Cr alloys in 1 N $H_2SO_4$ (pH 0) it was found that alloys containing more than 15 at% Cr show Cr-like behavior and alloys with a Cr concentration of below 10% behave similarly to Fe regarding their activation behavior [206]. Measurements of the critical current density of Fe–Cr (Cr: 0–16%) alloys in neutral sulfate solutions, on the other hand, show a linear dependence on the Cr concentration

[207]. Similar to this, no evidence for the existence of a critical Cr content was found in an investigation on the effect of the Cr content on the passivation behavior of Fe–*x*Cr–9%Ni alloys (Cr: 3.54–19.2%) [208] (Fig. 10). Later, other experimental evidence for the existence of a critical Cr concentration was provided and the findings were explained on the basis of the percolation model of passivation mentioned earlier [107, 108, 209].

*Stability of the oxide film*

The important influence of Cr addition into Fe is not only reflected by an enhanced passivation ability (i.e., decrease in the critical current density for passivation), but Cr also increases the protectiveness and stability of the passive film. This is reflected by the decrease in the passive current density in the polarization curves with increasing Cr content (Fig. 10). A surface analytical study of a series of Fe–Cr alloys indicates that the Cr content in the passive film formed in 1 N $H_2SO_4$ abruptly increases when the Cr content in the alloy is above 13% [210] (Fig. 11). The findings led to the conclusion that a Cr oxide concentration of more than 50% in the passive oxide film is required for stable passivity.

The investigation of anodic and cathodic dissolution of mixed $Fe_2O_3/Cr_2O_3$ films shows that a critical amount of $Cr_2O_3$ may prevent cathodic dissolution of the mixed oxide, and a sufficient amount of $Fe_2O_3$ can prevent anodic dissolution of the oxide layer [112] (Fig. 12). These critical concentrations strongly depend on the solution. Furthermore, an increase in the Cr content in binary Fe–Cr and ternary Fe–Cr–Ni additionally strongly increases the resistance against pitting corrosion as shown in Ref. [211] and by many others (Fig. 13).

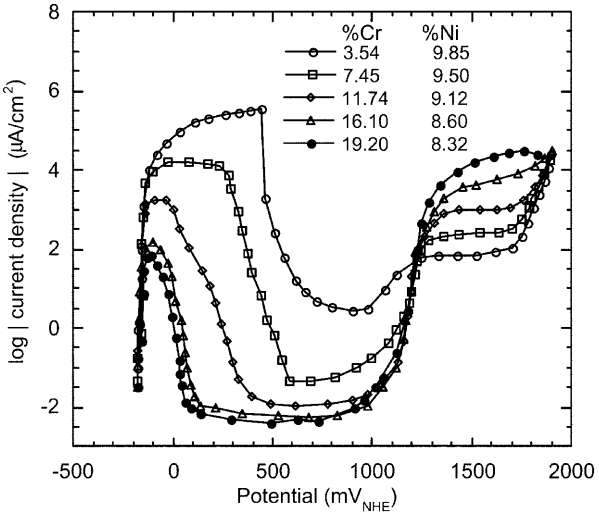


**Fig. 10** Anodic polarization curves for Fe–Cr–Ni alloys in 1 M $H_2SO_4$ (25 °C) (after Ref. [208])

*Chemical composition*

The chemical composition of the passive films on Fe–Cr alloys and stainless steels have been studied in great detail using surface analytical techniques. A widely accepted view on the composition of the films on Fe–Cr alloys is that the passive film of the Fe–Cr alloys is enriched with oxidized chromium species. Olefjord and Brox [212] found an average Cr content of 70% (the film consisting of $Cr^{3+}$, $Fe^{3+}$, and $Fe^{2+}$) in the passive film of a Fe–19Cr alloy formed in 0.5 M $H_2SO_4$. According to Hashimoto et al. [213] the passivity of ferritic stainless steels in 1 N HCl is due to the formation of a Cr-rich layer, which consists of a hydrated form of CrOOH and a minor amount of oxidized iron species.

The composition of the passive film on Fe–Cr alloys changes with the electrode potential. Okamoto [214] found that the passive film on AISI 304 steel formed in 1 N $H_2SO_4$ consisted mainly of chromium species at potentials lower than a critical potential $U = 400$ mV SCE; at higher potentials all Cr, Ni, and Fe were incorporated in the film. A similar result was reported by Olefjord and Brox [212], who found the amount of oxidized iron species in the film formed on the Fe–19Cr alloy in 1 N $H_2SO_4$ increased with increasing potential.

The oxidation state of iron is also affected by the potential. According to Clayton et al. [215], the passive film on the AISI 304 steel in 1 N $H_2SO_4$ consists of $Fe^{2+}$, $Fe^{3+}$, and $Cr^{3+}$ species at potentials lower than 0.4 V SCE; at higher potentials mainly $Fe^{3+}$ and $Cr^{3+}$ species were found in the film. Haupt and Strehblow [57]

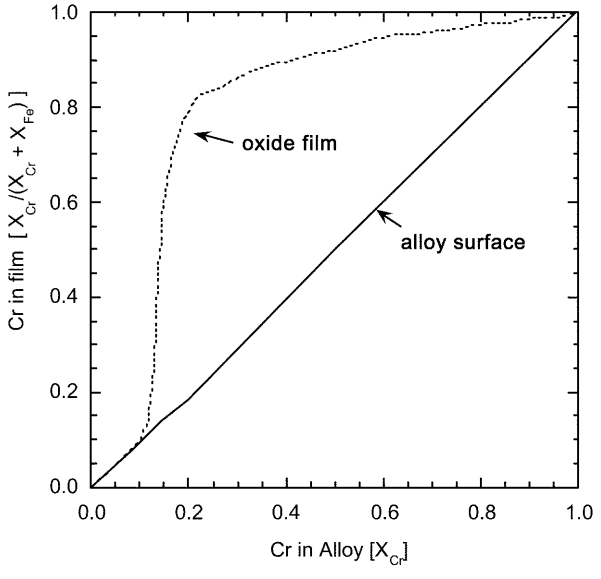


**Fig. 11** Changes in the cationic fraction of Cr in the passive film (*dashed line*) and the atomic fraction of Cr in the alloy surface below the passive film (*solid line*) on Fe–Cr alloys polarized at 100 and 500 mV SCE for 1 h in 1 N $H_2SO_4$ as a function of Cr in bulk alloys (after Ref. [210])

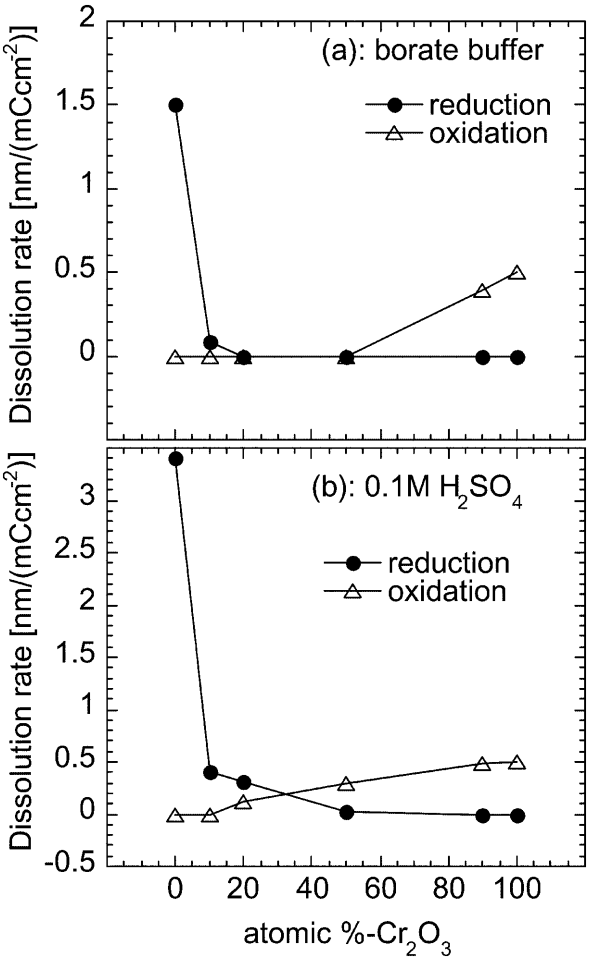


**Fig. 12** Electrochemical dissolution rate of mixed $Fe_2O_3/Cr_2O_3$ thin films (20 nm) as a function of the $Cr_2O_3$ content in the film during galvanostatic oxidation/reduction ($\pm 10$ μA/cm$^2$) in pH 8.4 borate buffer and in 0.1 M $H_2SO_4$ (after Ref. [112])

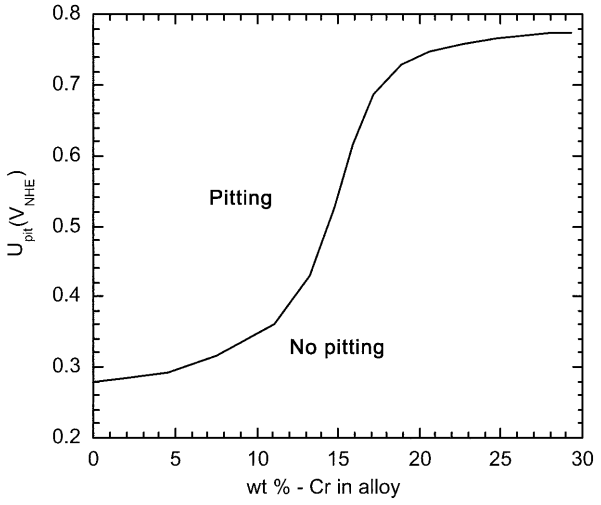


**Fig. 13** Pitting potentials for Fe–Cr–Ni alloys in 0.1 M NaCl at 25 °C (after Ref. [211])

accordingly found that the amount of $Fe^{3+}$ in the film increases with increasing potentials, but the oxidation of the ferrous species to ferric species does not occur completely in the passive film formed on Fe–Cr alloys in contrast to the behavior of pure iron. This could result from the formation of a highly resistive film on the Fe–Cr alloys, which inhibits the oxidation of iron, as Hashimoto et al. [213] postulate. On the other hand, later in situ studies on the passive film on pure iron in borate buffer indicate that even for films formed at high anodic potentials a small amount of $Fe^{2+}$ is present [179, 180]. The absence of $Fe^{2+}$ in the film found by ex situ techniques could therefore be an artefact induced by oxidation of the film in air after its removal from the electrolyte.

The composition of the passive film can vary in depth. $Cr^{3+}$ accumulation has often been found to take place in the inner part of the film [55, 57, 113, 212, 216, 217). According to Olefjord and Brox [212] the inner part of the passive film contains 100% $Cr^{3+}$. In the outer part additionally $Fe^{2+}$ and $Fe^{3+}$ species were found. At depth the oxygen was incorporated as $O^{2-}$, suggesting the inner Cr-rich layer consist of $Cr_2O_3$. In the outer layer the oxygen is present as $OH^-$ suggesting the layer to consisted of hydroxides and oxyhydroxides of iron and chromium.

Oxygen has been identified to be present in the passive film in three different metal–oxygen bonds: as an oxide *M*–O, a hydroxide *M*–OH, and an oxyhydroxide *M*–OOH. Nevertheless, no agreement exists on the details of the presence of hydrogen in the passive film. According to Okamoto [214] the passive film on Fe–Cr alloys is initially enriched with water as $H_2O$–*M*–$H_2O$ networks. With time, the film changes to a less hydrated structure, containing HO–*M*–OH and O–*M*–O bridges. According to Okamoto the bound water is exclusively associated with chromium compounds in the film. Clayton et al. [215] agree with Okamoto about the presence of bound water in the passive film but claim that it should be associated with the iron compounds in the film. In accordance with Okamoto, Clayton et al. found the amount of bound water in the film to decrease with ageing time.

For stainless steels, further investigations have been carried out to study the role of different alloying elements (mainly Ni and Mo) on the passivity and its breakdown. More information on the passive films on stainless steels can be found in recent reviews [66, 218].

### *Electronic properties*

The electronic properties of passive films on Fe base alloys and stainless steels have been, compared with the oxide films on Fe, much less investigated. Photoelectrochemical studies were carried out on binary Fe–Ni [82, 219] and Fe–Cr alloys [219, 220, 221], commercial ferritic Fe–Cr steels [90, 222, 223], and AISI 304 steel

(DIN 1.4301) [83, 99, 224, 225] and there is also work addressing the capacitance behavior of stainless steels [87, 214, 226, 227, 228, 229, 230].

In general, this work shows that with a low alloying element concentration the photocurrent and capacitance behavior of the passive films is similar to that of Fe. With increasing alloying element content, typically shifts in $U_{fb}$, an increase in $E_g$ as well as in Nd are observed, and the deviations from ideal semiconductor behavior become more pronounced.

Angelini et al. [82] observed by photopotential measurements on Fe–Ni alloys, for Ni contents below 40%, a behavior very similar to pure Fe. Kloppers et al. [220] investigated a series of Fe–Cr alloys and found the photocurrent to decrease with increasing Cr content between 5 and 30% Cr. All alloys showed n-type behavior with a negative shift of the optical flat-band potential with increasing Cr content. For all alloys, an indirect band-gap energy of 1.9 eV was found – identical to that of pure Fe – independent of the passivation potential, pH, and alloy composition. According to these authors the photocurrents decrease continuously with increasing Cr content – a fact that was taken as an indication that a distinct critical Cr content for high corrosion resistance [3, 107, 108, 231] does not exist.

Sunseri and coworkers [90, 222] investigated a series of ferritic Fe–Cr steels of the type 25Cr–4Ni–4Mo in a neutral 3.5% NaCl solution. For all the steels n-type behavior with optical flat-band potentials of 0 to –100 mV SCE was observed. Even though the composition of all the steels studied was very similar (Cr: 24.5–26%, Ni: 2.5–2.9%, Mo: 3.25–3.9% [222]), a different potential dependence of the band-gap energy was found for the different alloys. It was reported that generally $E_g$ decreases from 2.8 eV at –200 mV SCE to 2.0...2.5 eV (depending on the steel) at potential of 400 mV SCE followed by an increase in $E_g$ at higher potentials. The occurrence of this increase in the band-gap energy at 400 mV SCE, as well as the change in the phototransient behavior at this potential, was attributed by the authors to the contribution of nickel oxide surface states. In later investigations by others, however, this maximum in the band-gap energy was ascribed to the oxidation of the $Cr^{3+}$ in the passive film into $Cr^{6+}$ species [86].

Simoes and coworkers [83, 225] found for passive films on AISI 304 steel (DIN 1.4301) formed in pH 9.2 borate buffer at 800 mV SCE and subsequently polarized to lower potentials, a maximum photocurrent at 550 mV SCE. The indirect band-gap energy was found to be only slightly dependent on the potential (2.85 eV at 200 mV SCE; 2.7 eV at 800 mV SCE). The photocurrent spectra in the energy region below 3.1 eV was qualitatively discussed in terms of localized states.

DiPaola et al. [224] investigated AISI 304 steel (DIN 1.4301) in a neutral 1 M $NaClO_4$ solution. An evaluation of the photocurrent spectra revealed a strong potential dependence of the band-gap energy of 2.8 eV at 0 mV SCE down to 2.0 eV at 760 mV SCE and a significant change in the potential dependence was observed at 360 mV SCE. Other authors [85] attribute the nonideal behavior of the passive film on different steels to a defective (partially amorphous) structure of the film.

Gorse et al. [99] investigated passive films on AISI 304 steel (DIN 1.4301) in pH 9.2 borate buffer at 575 mV SCE, after exposure to $\alpha$ radiation for different times. The irradiation strongly increased the photocurrent response. The polarization curves of the irradiated samples in borate buffer and NaCl solution showed a pitting potential approximately 250 mV lower than samples that had not been irradiated. This led to the conclusion that irradiation strongly changes the defect structure of the passive film, and these defects increase the susceptibility of the material to pitting corrosion.

## Aluminium

The native oxide film formed on aluminium in water and in air at ambient temperatures is typically a few nanometers thick, consisting of $Al_2O_3$ [232, 233]. The film is generally described as amorphous. At higher temperatures, thicker films are formed, often consisting of a thin amorphous barrier layer and an outer crystalline layer. In boiling water the oxide film consists of AlOOH. Owing to the solubility of Al oxides in acidic and in alkaline solution, Al shows stable passivity only in the pH region of 4–9 (however, localized breakdown of passivity can take place in the presence of chloride ions). The $Al_2O_3$ layer formed on pure Al in air or in aqueous solutions acts as a dielectric. This makes it possible (as for other valve metals) to form thick anodic layers by anodic polarization to higher voltages.

Depending on the anodizing conditions, different type of oxide films can grow on Al. Dense, barrier-type oxide films up to the thickness of 0.1–1 μm are formed in solutions which hardly or only to a very minor extent dissolve Al oxides (e.g., borate, phosphate buffers). In solutions which chemically dissolve Al oxides (e.g., $H_2SO_4$) films up to 10–20-μm thick can grow. These thick films consist of an inner, pore-free barrier layer and an outer porous layer. The inner barrier layer is generally considered to consist of pure alumina, whereas the outer porous layer can contain species incorporated from the electrolyte solution [234, 235].

Formation of porous anodic films on Al has been review by Wood [236]. The pore size and the distribution obtained depend on the anodization conditions; the pore diameters typically vary between some and several 100 nm. Such porous alumina has recently found great interest as templates for the electrodeposition of nanostructures of different materials for the production of, for example, nanowires [237, 238]. Materials deposited in the pores include several metals and semiconductors; the principle is shown schematically in Fig. 14.

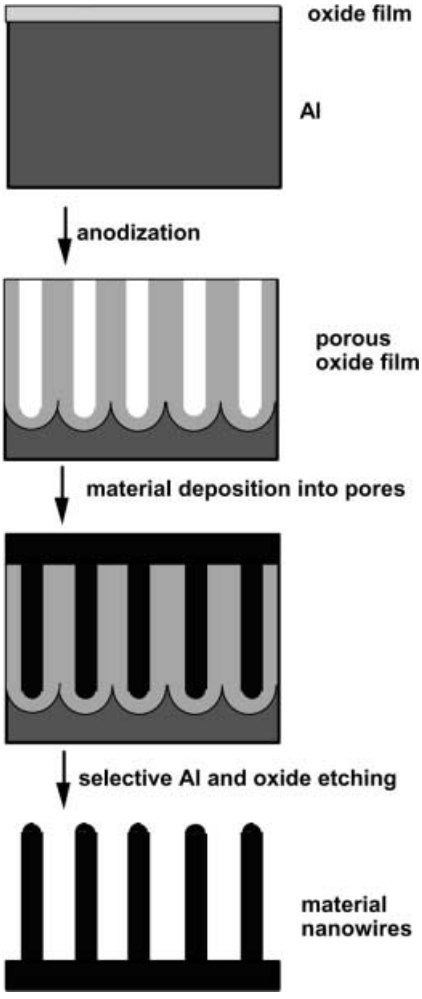


**Fig. 14** Exploiting regular pore arrays in anodized Al as templates for microfabrication. The sequence: a thick, porous oxide is grown by anodization; metal (or other material) is electrodeposited into the pores; the aluminium template is dissolved leaving nanowires of the deposited material behind

Oxide films on Al (native and anodic films) are often assumed to contain flaws which can play a crucial role in the corrosion behavior of passive Al acting as paths for cathodic and anodic current flow [233, 239, 240].

Many recent investigations on the nature of the oxide films formed on Al can be found in Ref. [241].

### Titanium

For titanium active uniform corrosion very seldom takes place owing to the excellent protection provided by the native film of $TiO_2$. Thermodynamically $TiO_2$ is very stable in the pH range between 2 and 12, and only complexing species such as HF or $H_2O_2$ lead to substantial dissolution [23]. Further, localized breakdown of passivity – mainly crevice corrosion of Ti – can take place at elevated temperatures (above 70 °C in seawater and above 315 °C in pure $H_2O$ [242, 243]).

The active/passive transition of Ti in $H_2SO_4$ of different concentrations has been discussed in Ref. [244]. It is interesting to note that even though the passivation potential of Ti is more negative than the equilibrium potential of hydrogen evolution and the critical current density is relatively low, Ti is not spontaneously passivated in deaerated strong acidic solutions. This is due to the relatively slow kinetics of the cathodic hydrogen evolution reaction on the Ti surface [245, 246]. This also explains the observation of depassivation leading to uniform corrosion of Ti in deoxygenated acidic media [244]. In oxidizing acids, however, Ti is spontaneously passive.

The majority of the investigations carried out on titanium are concerned with anodic oxide films formed under high anodic polarization. In these studies the growth kinetics and the properties of the anodic oxide films have been described. Anodization at high voltages thickens the native oxide films to several thousand angstroms, depending on the applied potential. Passive films on titanium formed at relatively low potentials (close to the open-circuit potential) are generally found to be amorphous in nature [247]. At higher potentials, a more crystalline film is formed [248, 249, 250]. Recrystallization is accompanied with the uptake of water and a rapider thickening of the oxide film with potential [247, 250]. For more details on the growth mechanism see Ref. [251].

The electronic properties of anodic films on titanium have extensively been studied, on one hand, because these films show a behavior perhaps most similar to an ideal semiconductor of all anodically formed films on metals and, on the other hand, $TiO_2$ is still being considered as one of the most promising materials in solar energy conversion. In fact, anodic $TiO_2$ films on Ti were found to behave very similarly to bulk $TiO_2$, i.e., an n-type semiconductor [252, 253, 254]. However, for anodic films properties such as the quantum yield or doping concentration can depend strongly on the formation conditions [255]. For a more detailed discussion on the electronic properties and the photoinduced growth on $TiO_2$ layers see Ref. [256] and references therein.

## Concluding remarks

Within the past 50 years the understanding of the mechanism of passivity and its breakdown has increased tremendously. This has been due mainly to extensive studies of a variety of relevant systems by numerous researchers tackling the field from different angles (materials science/technology, physics, chemistry, engineering). Almost any passive metal/environment combination expresses particular characteristics, making it difficult to reach a conclusive and ''universal'' understanding of the stability and protectiveness of passive films. New experimental approaches (e.g., using scanning techniques with a very high lateral resolution or

synchrotron radiation) led and lead to new insights, with regard to the optimization of the passivity of a material in a specific environment or to the fostering of the design of tailored materials for a novel application. Even though many questions remain open, and although past and present reflective thinkers are no doubt right when they state ''Rust never sleeps'' [257] recent science and technology has, we believe, at least in many technologically relevant areas, managed to force rust to take a nap.

## References


1. Bacon F (1861) In: Spedding J, Ellis RL, Heath DD (eds) The works of Francis Bacon, vol 5. Longman, London, p 359
2. Keating P (2000) Du scribe au savant. Presses Universitaires de France
3. Tomashov N (1966) Theory of corrosion and protection of metals. Macmillan, New York
4. Gmelin (1929–1932) Handbuch der Anorganischen Chemie, Teil 59A. Berlin
5. Keir J (1790) Philos Trans 80:359
6. Schönbein C (1836) Ann Phys Chem 37:390
7. Monnartz P (1911) Metallurgie 8:161
8. Bockris JO'M, Conway BE, Yeager E, White RE (eds) (1981) Comprehensive treatise of electrochemistry, vol 4. Plenum, New York
9. (1958) Z Elektrochem 62:619
10. (a) (1963) J Electrochem Soc 110; (b) (1964) J Electrochem Soc 111
11. (a) (1970) Electrochim Acta 15; (b) Electrochim Acta 16
12. Frankenthal RP, Kruger J (eds) (1978) The passivity of metals. The Electrochemical Society, Princeton, NJ
13. Froment M (ed) (1983) Passivity of metals and semiconductors. Elsevier, Amsterdam
14. Sato N, Hashimoto K (eds) (1990) Passivation of metals and semiconductors. Pergamon, Oxford
15. Heusler KE (ed) (1995) Mater Sci Forum 185–188
16. Ives MB, Luo JL, Rodda J (eds) (2000) Passivity of metals and semiconductors, Proceedings, vol 99-42. The Electrochemical Society, Pennington, NJ
17. Wilmsen CE (ed) (1985) Physics and chemistry of III-V compound semiconductor interfaces. Plenum, New York
18. Schmuki P, Sproule GI, Bardwell JA, Lu ZH, Graham MJ (1996) J Appl Phys 79:7303
19. Loorbeer P, Lorenz WJ (1978) In: Frankenthal RP, Kruger J (eds) The passivity of metals. The Electrochemical Society, Princeton, NJ, p 607
20. Epelboin I, Keddam M, Mattos OR, Takenouti H (1979) Corros Sci 19:1105
21. (a) Keddam M, Mattos OR, Takenouti H (1986) Electrochim Acta 31:1147; (b) Keddam M, Mattos OR, Takenouti H (1986) Electrochim Acta 31:1159
22. Vilche JR, Arvia A (1981) Anal Acad Nac Cs Ex Fis Nat Buenos Aires 33:33
23. Pourbaix M (1963) Atlas d'equilibres électrochimiques. Gautier-Vil lars & Cie, Paris
24. Diggle JW(1973) Oxides and oxide films. Dekker, New York
25. Chao CY, Lin L-F, Macdonald DD (1981) J Electrochem Soc 128:1187
26. Chao CY, Lin L-F, Macdonald DD (1982) J Electrochem Soc 129: 1874
27. Cabrera N, Mott NF (1948) Rep Prog Phys 12:267
28. Vetter KJ (1954) Z Electrochem Ber Bunsenges Phys Chem 58:230
29. Fehlner FP, Mott NF (1970) Oxid Met 2:59
30. Fromhold AT Jr (1976) In: Diggle JW, Vijh AK (eds) Oxides and oxide films, vol 3. Dekker, New York, p 1
31. Dewald JF (1955) J Electrochem Soc 102:1
32. Young L (1959) Can J Chem 37:276
33. Hauffe K, Illschner B (1954) Z Elektrochem 58:382
34. Lanyon AH, Trapnell BWW (1955) Proc R Soc Lond A 227:387
35. Eley DD, Wilkinson PR (1960) Proc R Soc Lond A 254:327
36. Green M (1960) Prog Semicond 4:37
37. Law JT (1958) J Phys Chem Solids 4:91
38. Sato N, Cohen M (1964) J Electrochem Soc 111:512
39. Kirchheim R (1987) Electrochim Acta 32:1619
40. Fehlner FP, Graham MJ (1995) In: Marcus P, Oudar J (eds) Corrosion mechanisms in theory and practice. Dekker, New York, p 123
41. Young L (1961) Anodic oxide films. Academic, New York
42. Arora MR, Kelly R (1977) J Electrochem Soc 124:1493
43. Ord JL, DeSmet DJ, Hopper MA (1976) J Electrochem Soc 123:1352
44. Ord JL, Clayton JC, DeSmet DJ (1977) J Electrochem Soc 124:1714
45. Wood GC, Brock AJ (1966) Nature 209:773
46. Parsons G, Wood GC (1969) Corros Sci 9:367
47. Wood GC, Khoo SW (1971) J Appl Electrochem 1:189
48. Wagner C (1933) Z Phys Chem B 21:25
49. Lohrengel MM (1993) Mater Sci Eng Rev 11:243
50. Pringle JPS (1979) Electrochim Acta 25:1423
51. Dignam MJ (1973) In: Diggle JW (ed) Oxides and oxide films, vol 1. Dekker, New York, p 143
52. MacDougall B, Mitchell DF, Graham MJ (1982) Corrosion 38:85
53. Hashimoto K, Osada K, Masumoto T, Shimodaira S (1976) Corros Sci 16:71
54. Mischler S, Vogel A, Mathieu HJ, Landolt D (1991) Corros Sci 32:925
55. Kirchheim R, Heine B, Fischmeister H, Hofmann S, Knote H, Stolz U (1989) Corros Sci 29:899
56. Castle JE, Qiu JH (1989) Corros Sci 29:591
57. Haupt S, Strehblow HH (1989) Corros Sci 29:163
58. Landolt D (1990) In: Isaacs HS, Bertocci U, Kruger J, Smialowska S (eds) Advances in localized corrosion. NACE, Houston, p 25
59. Mitchell DF, Graham MJ (1986) J Electrochem Soc 133:936
60. Hoppe HW, Strehblow HH (1989) Surf Interface Anal 14:121
61. Haupt S, Strehblow HH (1987) Langmuir 3:873
62. Maurice V, Yang WP, Marcus P (1998) J Electrochem Soc 45:909
63. Costa D, Yang WP, Marcus P (1995) Mater Sci Forum 185–188:325
64. Marcus P, Olefjord I (1979) Surf Interface Anal 4:29
65. Dongil K, Kagwade SW, Clayton CR (1998) Surf Interface Anal 26:155
66. Clayton CR, Olefjord I (1995) In: Marcus P, Oudar J (eds) Corrosion mechanisms in theory and practice. Dekker, New York, p 175
67. Olefjord I, Wegrelius L (1990) Corros Sci 31:89
68. Ryan MP, Newman RC, Thompson GE (1995) J Electrochem Soc 142:L177
69. Toney MF, Davenport AJ, Oblonsky LJ, Ryan MP, Vitus CM (1997) Phys Rev Lett 79:4282
70. Schultze JW, Lohrengel MM (2000) Electrochim Acta 45:2499
71. Krishnakumar R, Szklarska-Smialowska Z (1992). In: MacDougall BR, Alwitt RS, Ramanaraynan T (eds) Oxide films on metals and alloys. Proceedings, vol 92-22. The Electrochemical Society, Pennington, NJ, p 370
72. Schmuki P (1992) PhD thesis. Swiss Federal Institute of Technology, Zurich
73. Young EWA, Gerretsen H, de Wit KHW (1987) J Electrochem Soc 134:2257
74. Kofstad P, Lillerlund KP (1980) J Electrochem Soc 127: 2410
75. Young EWA, Stiphout PCM, de Wit KHW (1985) J Electrochem Soc 132:884
76. Metikos-Hukovis M, Ceraj-Ceric M (1987) J Electrochem Soc 134:2193
77. Searson PC, Latanision RM (1990) Electrochim Acta 35:445

78. Morrison SR (1980) Electrochemistry at semiconductor and oxidized metal electrodes. Plenum, New York
79. Stimming U, Schultze JW (1979) Electrochim Acta 24:859
80. Searson PC, Latanision RM, Stimming U (1988) J Electrochem Soc 135:1358
81. Wilhelm SM, Hackerman N (1981) J Electrochem Soc 128:1668
82. Angelini E, Maja M (1977) Chim Ind 59:420
83. Simoes AMP, Ferreira MGS, Rondot B, da Cunha Belo M (1990) J Electrochem Soc 137:82
84. DiPaola A, Shukla D, Stimming U (1991) Electrochim Acta 36:345
85. Schmuki P, Böhni H (1992) J Electrochem Soc 139:1908
86. Schmuki P, Böhni H (1994) J Electrochem Soc 141:362
87. Di Paola A (1989) Electrochim Acta 34:203
88. Stimming U (1986) Electrochim Acta 31: 415
89. Delnick FM, Hackerman N (1979) J Electrochem Soc 126:732
90. Sunseri C, Piazza S, DiPaola A, DiQuarto F (1987) J Electrochem Soc 134:2410
91. Chen CT, Cahan BD (1982) J Electrochem Soc 129:17
92. Cahan BD, Chen CT (1982) J Electrochem Soc 129:474
93. Leitner K, Schultze JW (1988) Ber Bunsenges Phys Chem 92:181
94. Koenig U, Schultze JW (1992) Solid State Ionics 53–56:255
95. Gerischer H (1989) Corros Sci 29:257
96. Gorse D, Rondot B, da Cunha Belo M (1990) Corros Sci 30:23
97. Hakiki NE, a Cunha Belo M, Simoes AMP, Ferreira MGS (1998) J Electrochem Soc 145:3821
98. Rajeshwar K, Peter LM, Fujishima A, Meissner D, Tomkiewich M (eds) (1997) Proceedings of the Symposium on Photoelectrochemistry. The Electrochemical Society, Pennington, NJ
99. Sato N (1998) Electrochemistry at metal and semiconductor electrodes. Elsevier, Amsterdam
100. Dean MH, Stimming U (1987) J Electroanal Chem 228:135
101. Gärtner WW (1959) Phys Rev 116:84
102. Leitner K, Schultze JW, Stimming U (1986) J Electrochem Soc 133:1561
103. Johnson EJ (1967) Semiconductors and semimetals, vol 3. Academic, New York, p 332
104. Gerischer H (1961) Z Phys Chem 27:48
105. Mott NF, Davis EA (1979) Electronic processes in non-crystalline Solids. Clarendon, Oxford
106. Mott NF (1966) Philos Mag 13:989
107. Sieradzki K, Newman RC (1986) J Electrochem Soc 133:1979
108. Qian S, Newman RC, Cottis RA, Sieradzki K (1990) J Electrochem Soc 137:435
109. Revesz AG, Kruger J (1978) In: Frankenthal RP, Kruger J (eds) The passivity of metals. The Electrochemical Society, Princeton, NJ, p 137
110. Sakashita M, Sato N (1978) In: Frankenthal RP, Kruger J (eds) The passivity of metals. The Electrochemical Society, Princeton, NJ, p 479
111. Clayton CR, Lu YC (1986) J Electrochem Soc 133:2465
112. Schmuki P, Virtanen S, Isaacs HS, Ryan MP, Davenport AJ, Böhni H, Stenberg T (1998) J Electrochem Soc 145:791
113. Brooks AR, Clayton CR, Doss K, Lu YC (1986) J Electrochem Soc 133:2459
114. Natishan PM, Isaacs HS, Janik-Czachor M, Macagno VA, Marcus P, Seo M (eds) (1998) Passivity and its breakdown. Proceedings, vol 97-26. The Electrochemical Society, Pennington, NJ
115. Böhni H (1987) Langmuir 3:924
116. ZsklarskaSmialowskaZ (1986) Pitting corrosion of metals. National Association of Corrosion Engineers, Houston
117. Strehblow HH (1995) In: Marcus P, Oudar J (eds) Corrosion mechanisms in theory and practice. Dekker, New York, p 201
118. Baroux B (1995) In: Marcus P, Oudar J (eds) Corrosion mechanisms in theory and practice. Dekker, New York, p 265
119. Frankel GS (1998) J Electrochem Soc 145:2186
120. Hine F, Komai K, Yamakawa K (eds) (1988) Localized corrosion. Elsevier, London
121. Tousek J (1985) Theoretical aspects of the localized corrosion of metals. TransTech, Rockport, Mass
122. Böhni H (1987) In: Mansfeld F (ed) Corrosion mechanisms. Dekker, New York, p 285
123. Brown BF, Kruger J, Staehle RW (eds) (1974) Localized corrosion. NACE, Houston
124. Frankenthal RP, Kruger J (eds) (1984) Equilibrium diagrams of localized corrosion. Proceedings, vol 84-9. The Electrochemical Society, Pennington, NJ
125. Isaacs HS, Bertocci U, Kruger J, Smialowska S (eds) (1990) Advances in localized corrosion. NACE, Houston
126. Natishan PM, Kelly RG, Frankel GS, Newman RC (eds) (1996) Critical factors in localized corrosion II. Proceedings, vol 95-15. The Electrochemical Society, Pennington, NJ
127. Schmuki P, Lockwood DJ, Bsiesy A, Isaacs HS (eds) (1997) Pits and pores: formation, properties, and significance for advanced luminescent materials. Proceedings, vol 97-7. The Electrochemical Society, Pennington, NJ
128. Canham LT (1990) Appl Phys Lett 57:1046
129. Cullis AG, Canham LT, Calcott PDJ (1997) J Appl Phys 82:909
130. Schmuki P, Erickson LE, Lockwood DJ (1998) Phys Rev Lett 80:4060
131. Sze SM (1983) VLSI Technology. McGraw-Hill, New York
132. Ikonopisov S (1977) Electrochim Acta 22:1077
133. Ikonopisov S, Girginov A, Machkova M (1979) Electrochim Acta 24:451
134. Montero I, Albella JM, Martinez-Duart JM (1985) J Electrochem Soc 132:814
135. Wood GC, Pearson C (1967) Corros Sci 7:119
136. Dyer CK, Leach JSL (1978) J Electrochem Soc 125:23
137. Tun Z, Noel JJ, Shoesmith DW (1999) J Electrochem Soc 146:988
138. Schmidt PF (1957) J Appl Phys 28:278
139. Schmidt PF (1968) J Electrochem Soc 115:167
140. Vermilyea DA (1956) J Appl Phys 27:963
141. Ward A, Damjanovic A, Gray E, O'Jea M (1976) J Electrochem Soc 123:1599
142. Zakzouk AM (1979) J Electrochem Soc 26:1772
143. Schultze JW, Stimming U (1975) Z Phys Chem 98:285
144. Laser D, Yaniv M, Gottesfeld S (1978) J Electrochem Soc 125:358
145. Lenzinger M, Snow EH (1969) J Appl Phys 40:278
146. Blesa MA, Morando PJ, Regazzoni AE (1994) Chemical dissolution of metal oxides. CRC, Boca Raton
147. Heusler KE (1978) In: Frankenthal RP, Kruger J (eds) The passivity of metals. The Electrochemical Society, Princeton, NJ, p 771
148. Plieth WJ, Vetter KJ (1969) Ber Bunsenges Phys Chem 73:1077
149. Heumann T, Rösener W (1955) Z Elektrochem 59:722
150. Niki K (1985) In: Bard AJ (ed) Standard potentials in aqueous solutions. Dekker, New York, p 453
151. Niki K, Tanaka N, Habashi E, Harfors WSH (1986) In: Bard AJ (ed) Encyclopedia of elements. Dekker, New York, p 255
152. Schmuki P, Virtanen S, Davenport AJ, Vitus CM (1996) J Electrochem Soc 143:3997
153. Schmuki P, Virtanen S, Davenport AJ, Vitus CM (1996) J Electrochem Soc 143:574
154. Schmuki P, Büchler M, Virtanen S, Isaacs HS, Ryan MP, Böhni H (1999) J Electrochem Soc 146:2097
155. Virtanen S, Schmuki P, Büchler M, Isaacs HS (1999) J Electrochem Soc 146:4087
156. Oblonsky LJ, Davenport AJ, Ryan MP, Isaacs HS, Newman RC (1996) In: Bardwell J (ed) Surface oxide films. Proceedings, vol 96-18. The Electrochemical Society, Pennington, NJ, p 223
157. Kaesche H (1979) Die Korrosion der Metalle. Springer, Berlin Heidelberg New York
158. Nagayama M, Cohen M (1962) J Electrochem Soc 109:781

159. Foley CL, Kruger J, Bechtold CJ (1967) J Electrochem Soc 114:994
160. Ord JL, Smet DJ (1976) J Electrochem Soc 123:1876
161. Haruyama S, Tsuru T (1976) Corros Sci 13:275
162. Rahner D, Forker W (1978) Z Phys Chem 18:344
163. Bardwell JA, MacDougall B, Graham MJ (1988) J Electrochem Soc 135:413
164. Sato N, Kudo K, Noda T (1970) Corros Sci 10:785
165. Ogura K, Majima T (1978) Electrochim Acta 23:1361
166. Ogura K, Sato K (1980) Electrochim Acta 25:857
167. Schroeder V, Devine TM (1999) J Electrochem Soc 146:4061
168. Seo M, Sato N, Lumsden JB, Staehle RW (1977) Corros Sci 17:209
169. Tjong SC, Yeager E (1981) J Electrochem Soc 128:2251
170. Büchler M, Schmuki P, Böhni H (1998) J Electrochem Soc 145:609
171. Davenport AJ, Oblonsky LJ, Ryan MP, Toney MF (2000) J Electrochem Soc 147:2162
172. Utaka I, Miyake S, Iimore T (1937) Nature 139:156
173. Mayne JEO, Pryor MJ (1949) J Chem Soc 1831
174. Cohen M (1952) J Phys Chem 56:451
175. O'Grady WE (1980) J Electrochem Soc 127:555
176. Oblonsky LJ, Devine TM (1995) Corros Sci 37:17
177. Long,GC, Kruger J, Black DR, Kuriyama M (1983) J Electrochem Soc 130:240
178. Davenport AJ, Sansone M (1995) J Electrochem Soc 142:725
179. Oblonsky LJ, Davenport AJ, Ryan MP, Isaacs HS, Newman RC (1997) J Electrochem Soc 144:2398
180. Büchler M, Schmuki P, Böhni H, Stenberg T, Mäntylä T (1998) J Electrochem Soc 145:378
181. Stimming U, Schultze JW (1976) Ber Bunsenges Phys Chem 80:1297
182. Wilhelm SM, Yun KS, Ballenger LW, Hackerman N (1979) J Electrochem Soc 126:419
183. Jantzen O (1965) Z Angew Phys 18:560
184. Quinn RK, Nasley RD, Banghman RJ (1976) Mater Res Bull 11:1011
185. Kennedy JH, Frese KW (1978) J Electrochem Soc 125:709
186. Kennedy JH, Frese KW (1978) J Electrochem Soc 125:723
187. Ord JL, Bartlett JH (1965) J Electrochem Soc 112:160
188. Wheeler D, Cahan BD, Chen CT, Yeager EB (1978) In: Frankenthal RP, Kruger J (eds) The passivity of metals. The Electrochemical Society, Princeton, NJ, p 546
189. Wisdom N, Hackerman N (1962) J Electrochem Soc 109:1067
190. Moshtev RV (1968) Ber Bunsenges Phys Chem 72:452
191. Allongue PH, Cachet H (1986) In: Gabrielli C (ed) Forum sur Les Impedance Electrochimiques. Montrouge, p 65
192. Cahan BD, Chen CT (1982) J Electrochem Soc 29:923
193. Stimming U (1983) In: Froment M (ed) Passivity of metals and semiconductors. Elsevier, Amsterdam, p 477
194. Grilikhes MS, Sapelova EV, Berezin MY, Gorlin AV, Sokolov MA, Sukhotin AM (1985) Elektrokhimiya 21:808
195. Searson P, Stimming U, Latanision RM (1986). In: McCafferty E, Brodd RJ (eds) Surfaces, inhibition and passivation. The Electrochemical Society, Princeton, NJ, p 175
196. Azumi K, Ohtsuka T, Sato N (1986) Trans Jpn Inst Met 27:382
197. König U, Lohrengel MM, Schultze JW (1987) Ber Bunsenges Phys Chem 91:426
198. Azumi K, Ohtsuka T, Sato N (1987) J Electrochem Soc 134:1352
199. Abrantes LM, Peter LM (1983) J Electroanal Chem150:593
200. Horowitz G (1983) J Electroanal Chem 159:421
201. Fredlein RA, Bard AJ (1979) J Electrochem Soc 126:1893
202. Schmickler W (1977) J Electroanal Chem 83:387
203. Stimming U (1979) PhD Thesis. Freie Universität Berlin, Berlin
204. Yanase A, Siratori K (1984) J Phys Soc Jpn 56:312
205. Froelicher M, Hugot-LeGoff A, Iovancicevic V (1983) In: Froment M (ed) Passivity of metals and semiconductors. Elsevier, Amsterdam, p 491
206. Rocha H-J, Lennartz G (1955) Arch Eisenhüttenwes 26:117
207. Uhlig HH, Woodside GE (1953) J Phys Chem 57:280
208. Osozawa K, Engell HJ (1966) Corros Sci 6:389
209. Fujimoto S, Newman RC, Smith GS, Kaye SP, Kheyrandish H, Colligon JS (1993) Corros Sci 35:51
210. Asami K, Hashimoto K, Shimodaira S (1978) Corros Sci 18:551
211. Horvath J, Uhlig HH (1968) J Electrochem Soc 115:791
212. Olefjord I, Brox B (1983) In: Froment M (ed) Passivity of metals and semiconductors. Elsevier, Amsterdam, p 561
213. Hashimoto K, Asami K (1979) Corros Sci 19:251
214. Okamoto G (1973) Corros Sci 13:471
215. Clayton CR, Doss K, Warren JB (1983) In: Froment M (ed) Passivity of metals and semiconductors. Elsevier, Amsterdam, p 585
216. Marcus P, Grimal JM (1992) Corros Sci 33:805
217. Lumsden JB, Stocker PJ (1983) In: Froment M (ed) Passivity of metals and semiconductors. Elsevier, Amsterdam, p 579
218. Streicher MA (2000) In: Revie RW (ed) Uhlig's corrosion handbook, 2nd edn. Wiley, New York, p 601
219. Angelini E, Maja M, Spinelli P (1977) J Phys C 5:261
220. Kloppers MJ, Bellucci F, Latanision RM (1991) In: Baer DR, Clayton CR, Davis GD (eds) Application of surface analysis methods to environmental/material interactions. Proceedings, vol 91-7. The Electrochemical Society, Pennington, NJ, p 287
221. Angelini E, Maja M (1977) Metal Ital 69:397
222. Di Paola A, Di Quarto F, Sunseri C (1986) Corros Sci 26:935
223. Di Paola A (1990) Corros Sci 31:739
224. Di Paola A, Shukla D, Stimming U (1991) Electrochim Acta 36:345
225. Simoes AMP, Ferreira MGS, Lorang G, da Cunha Belo M (1991) Electrochim Acta 36:315
226. Okamoto G, Shibata T (1970) Corros Sci 10:371
227. Sugimoto K, Sawada Y( 1977) Corros Sci 17:425
228. Curley-Fiorino ME, Schmid GM (1980) Corros Sci 20:313
229. Ferreira MGS, Dawson JL (1985) J Electrochem Soc 132:760
230. Harrison JA, Williams DA (1986) Electrochim Acta 31:1063
231. Newman RC, Meng FT, Sieradzki K (1988) Corros Sci 28:523
232 Ghali E (2000) In: Revie RW (ed) Uhlig's corrosion handbook, 2nd edn. Wiley, New York, p 677
233. Kaesche H (1978) In: Frankenthal RP, Kruger J (eds) The passivity of metals. The Electrochemical Society, Princeton, NJ, p 935
234. Diggle W, Downie TC, Goulding CW (1969) Chem Rev 365
235. Skeldon P, Shimizu K, Thompson GE, Wood GC (1985) Thin Solid Films 123:127
236. Wood GC (1974) In: Diggle JW (ed) Oxides and oxide films, vol 2. Dekker, New York, p 148
237. Masuda H, Fukuda K (1995) Science 268:1466
238. Li A-P, Müller F, Birner A, Nielsch K, Gösele U (1998) J Appl Phys 84:6023
239. Wood GC, Sutton WH, Richardson JA, Riley TNK, Malherbe AG (1974) In: Staehle R, Brown B, Kruger J, Agrawal A (eds) Localized corrosion. NACE-3. NACE, Houston, p 526
240. Wood GC, Richardson JA, Abd Rabbo MF, Mapa LB, Sutton WH (1978) In: Frankenthal RP, Kruger J (eds) (1978) The passivity of metals. The Electrochemical Society, Princeton, NJ, p 973
241. Hebert KR, Thompson GE (eds) (1994) Oxide films on metals and alloys VII. Proceedings, vol 94-25. The Electrochemical Society, Pennigton, NJ
242. Hughes PC, Lamborn IR (1961) J Inst Met 89:1960
243. Schutz RW, Thomas DE (1987) Metals handbook, 9th edn, vol 13. ASM International. Metals Park, Ohio
244. Brauer E, Nann E (1969) Werkst Korros 20:676
245. Stern M, Wissemberg W (1959) J Electrochem Soc 106:756
246. Straumanis ME, Shih ST, Schlechten AW (1955) J Phys Chem 59:317
247. Shibata T, Zhu Y-C (1994) Corros Sci 36:153
248. Leach JSL, Pearson BR (1988) Corros Sci 28:43
249. Shibata T, Zhu YC (1995) Corros Sci 37:253

250. Ohtsuka T, Masuda M, Sato N (1985) J Electrochem Soc 132:787
251. Schultze JW, Lohrengel MM, Ross D (1983) Electrochim Acta 28:973
252. Heusler KE, Yun KS (1977) Electrochim Acta 27:977
253. Quinn RK, Armstrong NR (1978) J Electrochem Soc 125:1790
254. Dutoit EC, Cardon F, Gomes WP (1976) Ber Bunsenges Phys Chem 80:1285
255. Müller Y, Virtanen S (2000) In: Ives MB, Luo JL, Rodda J (eds) Passivity of metals and semiconductors, Proceedings, vol 99-42. The Electrochemical Society, Pennington, NJ, p 128
256. Schultze JW, Kudelka S, Davepon B, Krumm R (1998) In: Natishan PM, Isaacs HS, Janik-Czachor M, Macagno VA, Marcus P, Seo M (eds) Passivity and its breakdown. Proceedings, vol 97-6. The Electrochemical Society, Pennington, NJ, p 726
257. Young N (1978) Warner Records